Ikuta K. and Nakaya T.,	SARS-CoV spike protein into viral particles due to amino acid substitutions within the receptor binding domain	*Dis.*			
Wu, X.; Iguchi, T.; Itoh, N.; Okamoto, K.; Takagi, T.; Tanaka, K.; Nakanishi, T.	Ascorbic Acid transported by sodium-dependent vitamin C transporter 2 stimulates steroidogenesis in human choriocarcinoma cells	*Endocrinology*	149	73–83	2008
Nishikiori, R.; Makino, Y.; Ochi, Y.; Yamashita,Y.; Okamoto, K.; Kawashita, N.; Takahara, J.; Yasunaga, T.; Takagi, T.; Kawase, M.	Development of Fingerprint Verification Type Self-Organized Map Applied to Profiling Seized Methamphetamine	*J. Comput. Aided Chem.*	9	30–36	2008
Goto, N.; Kurokawa, K.; Yasunaga T.	Analysis of invariant sequences in 266 complete genomes	*Gene*	401	172–180	2007
Lapp, H.; Bala, S.; Balhoff, J. P.; Bouck, A.; Goto, N.; Holder, M.; Holland, R.; Holloway, A.; Katayama, T.; Lewis, P. O.; Mackey, A. J.; Osborne, B. I.; Piel, W. H.; Kosakovsky Pond, S. L.; Poon, A. F. Y.; Qiu, W.-G.; Stajich, J. E.; Stoltzfus, A.; Thierer, T.; Vilella, A. J.; Vos, R. A.; Zmasek, C. M.; Zwickl, D. J.; Vision, T. J.	The 2006 NESCent Phyloinformatics Hackathon: a field report	*Evolutionary Bioinformatics*	3	357–366	2007
Nishikiori, R.; Yamaguchi, M.; Takano, K.; Enatsu, T.; Tani, M.; de Silva, U. C.; Kawashita, N.; Takagi, T.; Morimoto, S.; Hangyo, M.; Kawase, M.	Application of partial least square on quantitative analysis of L-, D-, and DL-tartaric acid by terahertz absorption spectra	*Chem. Pharm. Bull.*	56	305–307	2007
Ogawa K., Sonoyama T.,	Roles of Shortly Connecting	*Extremophiles*	6	797–807	2007

Takeda T., Ichiki S., Nakamura S., Kobayashi Y., Uchiyama S., Nakasone K., Takayama S., Mita H., Yamamoto Y., and Sambongi Y.,	Disulfide Bond in the Protein Stability and Function of Shewanella violacea Cytochrome c_5, Redox				
Takahashi R., Nakamura S., Yoshida T., Kobayashi Y., and Ohkubo T.,	Crystallization of human nicotinamide phosphoribosyltransferase.	*Acta Crystallogr.*	*F63*	375–377	2007
Lin L., Nakano H., Nakamura S., Uchiyama S., Fujimoto S., Matsunaga S., Kobayashi Y., Ohkubo T., and Fukui K.,	Crystal Structure of Pyrococcus horikoshii PPC Protein at 1.60 Å Resolution.	*Proteins*	67	505–507	2007

Ⅳ．研究成果の刊行物・別刷（抜粋）

1．**Electrostatically constrained alpha-helical peptide inhibits replication of HIV-1 resistant to enfuvirtide**

Nishikawa, H.; Nakamura, S.; Kodama, E.; Ito, S.; Kajiwara, K.; Izumi, K.; Sakagami, Y.; Oishi, S.; Ohkubo, T.; Kobayashi, Y.; Otaka, A.; Fujii, N.; Matsuoka, M.

Int. J. Biochem. Cell. Biol., **41**, 891–899, (2009).

2．**Phenotypic studies on recombinant human immunodeficiency virus type 1 (HIV-1) containing CRF01_AE env gene derived from HIV-1-infected patient, residing in central Thailand.**

Utachee, P.; Jinnopat, P.; Isarangkura-Na-Ayuthaya, P.; de Silva, U.C.; Nakamura,S.; Siripanyaphinyo, U.; Wichukchinda, N.; Tokunaga, K.; Yasunaga, T.; Sawanpanyalert, P.; Ikuta, K.; Auwanit, W.; Kameoka, M.

Microbes Infect., **11**, 334–343, (2009).

1．**Enhancement of Ordinal CoMFA by Ridge Logistic Partial Least Squares**

Ohgaru, T., Shimizu, R., Okamoto, K., Kawashita, N., Kawase, M., Shirakuni, Y., Nishikiori, R., Takagi, T.

J. Chem. Inf. Model. **48**, 910–917, (2008).

The International Journal of Biochemistry & Cell Biology 41 (2009) 891–899

Contents lists available at ScienceDirect

The International Journal of Biochemistry & Cell Biology

journal homepage: www.elsevier.com/locate/biocel

Electrostatically constrained α-helical peptide inhibits replication of HIV-1 resistant to enfuvirtide

Hiroki Nishikawa[a], Shota Nakamura[b], Eiichi Kodama[c,*], Saori Ito[a], Keiko Kajiwara[c,d], Kazuki Izumi[c], Yasuko Sakagami[c], Shinya Oishi[a], Tadayasu Ohkubo[e], Yuji Kobayashi[f], Akira Otaka[g], Nobutaka Fujii[a], Masao Matsuoka[c]

[a] Graduate School of Pharmaceutical Sciences, Kyoto University, Sakyo-ku, Kyoto 606-8501, Japan
[b] Research Institute for Microbial Diseases, Osaka University, Suita, Osaka 565-0871, Japan
[c] Laboratory of Virus Control, Institute for Virus Research, Kyoto University, Sakyo-ku, Kyoto 606-8507, Japan
[d] Institute for Virus Research, and Graduate School of Biostudies, Kyoto University, Sakyo-ku, Kyoto 606-8507, Japan
[e] Graduate School of Pharmaceutical Sciences, Osaka University, Suita, Osaka 565-0871, Japan
[f] Osaka University of Pharmaceutical Sciences, Takatsuki, Osaka 569-1094, Japan
[g] Graduate School of Pharmaceutical Sciences, The University of Tokushima, Tokushima 770-8505, Japan

ARTICLE INFO

Article history:
Received 7 July 2008
Received in revised form 19 August 2008
Accepted 22 August 2008
Available online 10 September 2008

Keywords:
HIV
Fusion
Peptide
Inhibitor
α-Helix

ABSTRACT

α-Helical peptides, such as T-20 (enfuvirtide) and C34, derived from the gp41 carboxyl-terminal heptad repeat (C-HR) of HIV-1, inhibit membrane fusion of HIV-1 and the target cells. Although T-20 effectively suppresses the replication of multi-drug resistant HIV variants both in vitro and in vivo, prolonged therapy with T-20 induces emergence of T-20 resistant variants. In order to suppress the emergence of such resistant variants, we introduced charged and hydrophilic amino acids, glutamic acid (E) and lysine (K), at the solvent accessible site of C34. In particular, the modified peptide, SC34EK, demonstrates remarkably potent inhibition of membrane fusion by the resistant HIV-1 variants as well as wild-type viruses. The activity was specific to HIV-1 and little influenced by serum components. We found a strong correlation between the anti-HIV-1 activities of these peptides and the thermostabilities of the 6-helix bundles that are formed with these peptides. We also obtained the crystal structure of SC34EK in complex with a 36 amino acid sequence (N36) comprising the amino-terminal heptad repeat of HIV-1. The EK substitutions in the sequence of SC34EK were directed toward the solvent and generated an electrostatic potential, which may result in enhanced α-helicity of the peptide inhibitor. The 6-helix bundle complex of SC34EK with N36 appears to be structurally similar to that of C34 and N36. Our approach to enhancing α-helicity of the peptide inhibitor may enable future design of highly effective and specific HIV-1 inhibitors.

1. Introduction

Enfuvirtide (T-20), which has been clinically approved as the first fusion inhibitor of HIV-1, is derived from a 36 amino acid region of the carboxyl-terminal heptad repeat (C-HR) of gp41, an HIV-1 transmembrane envelope glycoprotein, which plays central role in the fusion of HIV-1 with host cells. T-20 prevents the formation of a 6-helix bundle, which is comprised of a trimer of dimers formed from the amino-terminal heptad repeat (N-HR) and the carboxyl-terminal heptad repeat (C-HR) in an antiparallel orientation. Six-helix formation by physiological gp41 enables host cell and virus membranes to contact and fuse, enabling the virus entry into the cells. Therefore, inhibition of the formation of this 6-helix bundle prevents fusion of HIV-1 and targeted host cell membranes (Derdeyn et al., 2000; Wild et al., 1992). Notably, T-20 effectively suppresses the replication of HIV-1 variants, which are resistant to multiple reverse transcriptase and protease inhibitors, and has been used in the optimized regimens for HIV-1-infected patients harboring multi-drug resistant HIV-1 variants (Lalezari et al., 2003; Lazzarin et al., 2003).

Emergence of T-20-resistant HIV-1 was reported not only in patients receiving T-20 monotherapy in a phase I clinical trial (Wei et al., 2002), but also in patients treated with a combination of T-20

* Corresponding author at: 53 Kawaramachi Shogoin, Sakyo-ku, Kyoto 606-8507, Japan. Tel.: +81 75 751 3986; fax: +81 75 751 3986.
E-mail address: ekodama@virus.kyoto-u.ac.jp (E. Kodama).

1357-2725/$ – see front matter © 2008 Elsevier Ltd. All rights reserved.
doi:10.1016/j.biocel.2008.08.039

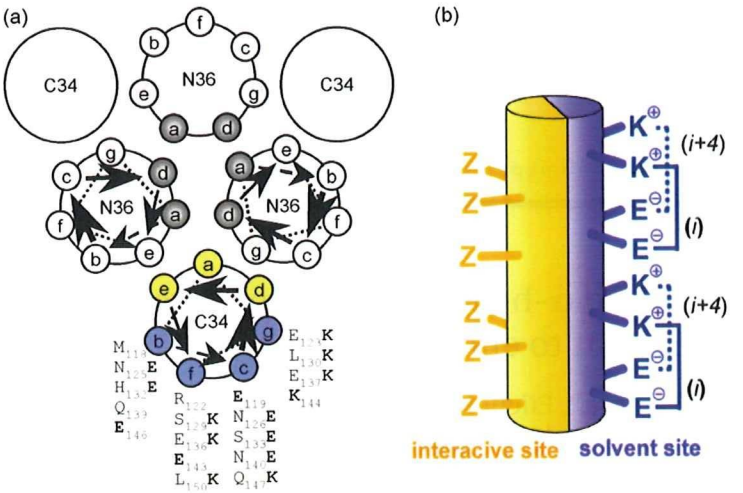

Fig. 1. Helical wheel representation of the 6-helix bundle structure and the design of SC34EK. (a) Amino acid residues at positions a, d, e of C34 are interactive sites that form the 6-helix complex with N36, while the remaining amino acid residues at positions b, c, f, g are solvent accessible sites, which are substituted with Glu (E) or Lys (K) in SC34EK. (b) The design concept of introducing the EK motif to the solvent accessible site. The α-helical C-HR peptide could be divided into interactive (red) and solvent (blue) sites. Z indicates the original amino acids of C34. Only amino acid residues at solvent sites were replaced by E at the *i* position and K at the *i* + 4 position.

and other inhibitors in subsequent phases II and III trials (Matthews et al., 2004; Poveda et al., 2002). These resistant variants frequently acquired mutations in gp41, especially in amino acids 36–45 of the N-HR region (Aquaro et al., 2006; Cabrera et al., 2006; Mink et al., 2005; Poveda et al., 2002; Rimsky et al., 1998; Wei et al., 2002) (Fig. 1). Additionally, complementary mutations in the C-HR region, such as S138A mutation, were found in some T-20 resistant variants (Cabrera et al., 2006; Poveda et al., 2004; Xu et al., 2005). Introduction of these complementary mutations compensates for impaired HIV-1 replication stemming from the primary mutations that give rise to resistance. The N43D mutation in the N-HR region that confers resistance to T-20 is a well documented example (Xu et al., 2005).

Although T-20 inhibits gp41-mediated fusion (Derdeyn et al., 2000; Wild et al., 1992), it has additional effects on HIV-1 replication. For instance, baseline sensitivity of HIV-1 to T-20 is influenced not only by the amino acid sequence of gp41, but also by the co-receptor specificity (CCR5/CXCR4) defined by the structure of the V3 loop of gp120, a glycoprotein capping gp41, which binds to the CD4 cells (Derdeyn et al., 2000; Derdeyn et al., 2001). Moreover, substitutions within the CD4 binding domain of gp120 also contribute to the resistance of the virus to T-20 (Baldwin and Berkhout, 2006). Thus, the mode of action and the mechanism of resistance to T-20 seem to be complicated. In contrast, another fusion inhibitor known as C34, has been clearly shown to bind to the N-HR in vitro and act as a decoy of gp41 C-HR and prevent the formation of the 6-helix bundle (Chan et al., 1997; Liu et al., 2005; Xu et al., 2007). Its inhibitory effect is over 10-fold greater than that of T-20 (Armand-Ugon et al., 2003; Nameki et al., 2005). Thus, C34 appears to be a suitable peptide to employ in the rational design of an improved HIV fusion inhibitor, based on the interaction between the peptide and the target.

It has been reported that α-helicity of the C-HR and N-HR peptide complexes correlates with the anti-HIV-1 activity of the peptide inhibitor (Chan et al., 1998), suggesting that enhancement of α-helicity of C34 may provide higher affinity to the N-HR region, thus resulting in more potent anti-HIV-1 activity. To design potent fusion inhibitors using the enhancement of α-helicity approach, we divided the α-helical peptide C34 into two characteristic interactive (a, d, e) and solvent accessible (b, c, f, g) sites according to the reported N36/C34 structure (Fig. 1) (Chan et al., 1997). When HIV-1 gp41 is folded, a tryptophan-rich domain (WRD) in the N-terminus of C-HR plays an important role in tight and specific binding, through the interaction of the hydrophobic aromatic ring with a deep groove formed by the N-HR coiled coil (Chan and Kim, 1998; Salzwedel et al., 1999). In fact, C34 contains the N-terminal WRD, which binds to a hydrophobic pocket formed by the amino acid residues L57, W60 and K63 on the N-HR trimer surface (Chan et al., 1998; Ferrer et al., 1999), resulting in higher anti-HIV-1 activity of C34 compared to T-20, which lacks the N-terminal WRD. On the other hand, the solvent accessible site appears to contribute little to the formation of the 6-helix bundles, as demonstrated by the crystal structure of C34 bound to N36 (Chan et al., 1997). Therefore, amino acids in the interactive site are indispensable for binding, whereas those in the solvent accessible site may be replaceable (Fig. 1). To enhance the α-helicity of C34, we introduced a series of systematic replacements of amino acid residues in the solvent accessible site, where the original amino acid residues were substituted with charged and hydrophilic glutamic acid (E) or lysine (K) with the intention of forming possible intrahelical salt-bridges (Marqusee and Baldwin, 1987) (Fig. 1b). We obtained two peptides, SC34 and SC34EK (Fig. 2a), both of which gratifyingly demonstrated increased anti-HIV-1 activity (Otaka et al., 2002).

In this study, we demonstrate that SC34EK maintains highly potent activity against T-20 resistant clones of HIV-1, as well as several clinical isolates, and we reveal that the enhanced α-helicity of SC34EK is indeed involved in the improvement of activity. The activities are specific to HIV-1 and are not influenced by serum components. Structural analysis indicates that electrostatic interactions introduced by EK substitutions enhance the conformational stability of the 6-helix bundle, thus preventing HIV-1 fusion with the host cell. The information from our investigations involving the enhanced α-helicity of SC34EK should enable further design of highly effective and specific HIV-1 inhibitors.

2. Materials and methods

2.1. Cells and viruses

MT-2 and 293T cells were grown in RPMI1640- and Dulbecco's modified Eagle medium (DMEM)-based culture medium, respec-

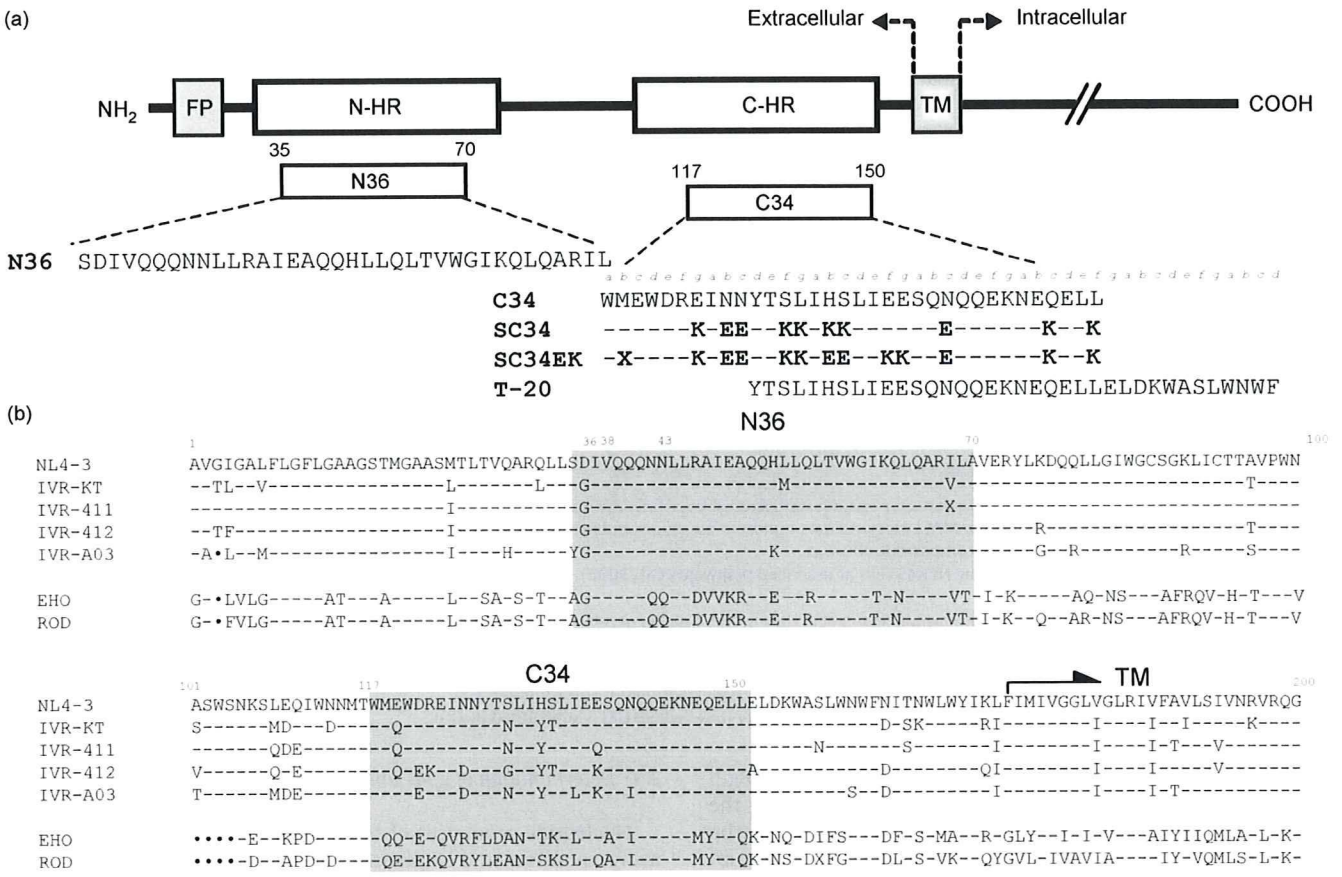

Fig. 2. Schematic view of gp41 and C34 derivatives and amino acid alignment of gp41. (a) The locations of the fusion peptide (FP), the amino-terminal heptad repeat region (N-HR), the carboxyl-terminal heptad repeat region (C-HR), and the transmembrane domain (TM) and the amino acid sequences of N36, T-20, C34 and its derivatives are shown. The residue numbers of each peptide correspond to their positions in gp41 of the NL4-3 strain. The X in SC34EK indicates norleucine, introduced to avoid oxidation of the methionine residues. No differences between the original methionine- and norleucine-containing peptide were observed (Otaka et al., 2002). (b) Alignment of amino acid sequence of clinical isolates (KT, IVR411, IVR412 and IVR-A03; GenBank accession number; AB222704, AB222705, AB222706 and AB222703, respectively) and HIV-2 strains (EHO and ROD) are shown. Corresponding regions of N36 and C34 are indicated in gray. Identical or deleted amino acids from the sequence of NL4-3 are indicated with a bar or a dot, respectively. The X in amino acid sequences of IVR411 and ROD indicates the mixture of I and V for IVR411, and mixture of I and M for ROD.

tively. HeLa-CD4-LTR-β-gal cells were kindly provided by Dr. M. Emerman through the AIDS Research and Reference Reagent Program, Division of AIDS, National Institute of Allergy and Infectious Disease (NIAID) (Bethesda, MD) and were used for the drug susceptibility assay (MAGI assay) as described previously (Kimpton and Emerman, 1992; Kodama et al., 2001; Maeda et al., 1998). The activity of test compounds was determined as the concentration that blocked HIV-1 replication by 50% (EC_{50}).

Laboratory HIV-1 (III_B) and HIV-2 (EHO and ROD) strains were used. An HIV-1 infectious clone pNL4-3 was used for constructions and for the production of HIV-1 variants as described (Nameki et al., 2005). A wild-type HIV-1, HIV-1_{WT}, was generated by transfection of pNL4-3 into 293T cells. Clinical isolates obtained from drug-naïve and heavily drug-experienced patients, were kindly provided by Dr. S. Oka (AIDS Clinical Center, International Medical Center of Japan, Tokyo, Japan). Their co-receptor tropisms were determined using NCK45 cells as described previously (Kajiwara et al., 2006).

2.2. Antiviral agent

The peptide-based fusion inhibitors used in this study were synthesized as described previously (Otaka et al., 2002), and the sequences can be identified in Fig. 2a. 3′-Azido-3′-deoxythymidine (AZT) and 2′,3′-dideoxycytidine (ddC) were purchased from Sigma (St. Louis, MO, USA). MKC-442 was provided by Dr. S. Shigeta (Fukushima Medical University, Fukushima, Japan).

2.3. Determination of drug susceptibility of HIV-1

The peptide sensitivity of infectious clones was determined using the MAGI assay with as described previously (Kodama et al., 2001; Maeda et al., 1998). The activity of test compounds was determined as the concentration that blocks HIV-1 replication by 50% (EC_{50}). For clinical isolates, PHA-stimulated peripheral blood mononuclear cells (PBMCs) were used as described previously (Kodama et al., 2001). PBMCs (10^6 cells/ml) were exposed to test compounds and HIV-1, and were cultured in the presence of interleukin 2 for 7 days. Amounts of p24 protein in the supernatants of the cultures were then determined using the commercially available p24 antigen enzyme linked solvent assay kit.

2.4. Construction of recombinant HIV-1 clone

Recombinant infectious HIV-1 clones with substituted V3 regions, pNL-$V3_{ADA}$ and pNL-$V3_{SF162}$ were generated using pNL4-3. The V3 region, corresponding to n.t. 7029–7249 of pNL4-3, was amplified using primers containing appropriate BglII and NheI restriction enzyme cleavage sites for directional cloning into pBS-

Table 1
Antiviral activity of gp41-derived peptides against gp41 and gp120 V3 recombinant virus[a]

Clone	Tropism[b]	EC_{50} (nM)					
		ddC	N36	T-20	C34	SC34	SC34EK
gp41 recombinant virus							
WT[c]		404 ± 196	180 ± 70	35 ± 17	3.2 ± 0.9	1.4 ± 0.7	0.7 ± 0.3
L33S		289 ± 24	39 ± 11	**>1000**	2.9 ± 0.9	1.3 ± 0.1	0.9 ± 0.3
V38A		714 ± 109	407 ± 76	**402 ± 68**	**96 ± 29**	2.0 ± 0.5	1.1 ± 0.6
V38E		291 ± 57	41 ± 14	**>1000**	**492 ± 85**	**37 ± 12**	**4.3 ± 1.3**
N43K		321 ± 8.5	234 ± 63	114 ± 19	**50 ± 9.5**	2.5 ± 0.3	2.7 ± 0.3
N43D		430 ± 42	461 ± 266	**>1000**	**>100**	**9.0 ± 6.6**	1.0 ± 0.8
D36S/V38M		296 ± 88	178 ± 31	42 ± 6.4	7.2 ± 4.0	1.9 ± 0.1	0.8 ± 0.3
V38E/N42S		273 ± 105	227 ± 20	**>1000**	**322 ± 7.5**	**32 ± 3.1**	3.2 ± 1.0
ΔFNSTW/L33S/N43K[d]		276 ± 39	152 ± 31	**>1000**	**248 ± 56**	2.7 ± 0.3	**4.4 ± 0.5**
ΔFNSTW/D36G/I37K/N126K/L204I[d]		246 ± 67	547 ± 7.8	**754 ± 174**	**67 ± 21**	4.6 ± 0.9	2.9 ± 0.8
gp120 V3 recombinant virus							
V3-ADA	R5	362 ± 102	360 ± 91	**289 ± 19**	6.8 ± 3.3	0.7 ± 0.4	2.0 ± 0.2
V3-SF162[e]	R5	995 ± 219	383 ± 9.9	19 ± 2.8	7.8 ± 3.5	0.5 ± 0.2	0.5 ± 0.2
V3-CH1[f]	R5X4	649 ± 4.5	**2207 ± 42**	16 ± 1	5.6 ± 0.1	1.3 ± 0.1	0.7 ± 0.1
V3-CH2[g]	R5	1515 ± 177	192 ± 13	35 ± 32	3.8 ± 0.1	0.4 ± 0	0.9 ± 0.8

[a] Anti-HIV-1 activity was determined using the MAGI assay. All data represent means ± standard deviation obtained from the results of three independent experiments. Bold indicates over 5-fold increase in EC_{50} value compared to HIV-1_{WT}.

[b] The co-receptor tropism was determined using NCK45 cells as described (Kajiwara et al., 2006).

[c] HIV-1_{NL4-3} served as a wild-type virus.

[d] ΔFNSTW is the deletion of five amino acids at position 364–368 in the gp120 V4 region of HIV-1_{NL4-3} (Nameki et al., 2005). Fusion inhibitor resistant variants used have been previously reported (Armand-Ugon et al., 2003; Nameki et al., 2005).

[e] The V3 region of NL4-3 gp120 was replaced with the corresponding region of HIV-1_{SF162}.

[f] HIV-$1_{V3\text{-}CH1}$ has mutations in the gp120 V3 region of primary isolate HIV-1_{KMT}, where GKI is substituted by GEI.

[g] HIV-$1_{V3\text{-}CH2}$ has mutation in the gp120 V3 region of the primary isolate HIV-1_{KMT}, where GKI is substituted by GQI.

$gp120_{WT}$. The resulting amplified V3 region was subjected to BglII and NheI digestion, subcloned into pBS-$gp120_{WT}$ containing the corresponding region in the DNA fragment of EcoRI–NheI (1510 bp containing gp120 V1, V2 and V3, n.t. 5740–7249 of pNL4-3) and subsequently ligated into pNL4-3. pNL-$V3_{CH1}$ and $V3_{CH2}$, CCR5 and dual (CXCR4 and CCR5) tropic molecular clones, were kindly donated by Dr. Y. Maeda, Kumamoto University (Kumamoto, Japan) (Foda et al., 2001; Maeda et al., 2000).

Recombinant infectious HIV-1 clones carrying various mutations in gp120 and/or gp41 were also generated using pNL4-3. Briefly, the desired mutations were introduced using site directed mutagenesis into the region of pSL-$gp41_{WT}$ flanked by the NheI–BamHI restriction enzyme sites (1220 bp containing gp120 V4, V5 and gp41 ectodomain n.t. 7250–8469 of pNL4-3) (Weiner et al., 1994). After restriction enzyme digestion and purification the NheI–BamHI fragments were ligated into pNL4-3, generating a series of molecular clones with the desired mutations.

Each molecular clone was transfected into 293T cells (10^5 cells/6-well culture plate). After 48 h, MT-2 cells (10^6 cells/well) were added and co-cultured with the 293T cells for an additional 24 h. When an extensive cytopathic effect was observed, the supernatants were harvested and stored at −80 °C for further use.

Table 2
Antiviral activity of gp41-derived peptides against clinical isolates[a]

Strain	EC_{50} (nM)				
	AZT	T-20	C34	SC34	SC34EK
NL4-3 (WT)[b]	2.0	36	3.2	0.36	0.4
KT (WT)[b]	2.0	11	0.2	0.1	0.03
IVR411	**7600**	4.1	0.2	3.1	0.04
IVR412	**9060**	23	7.2	**4.8**	0.1
IVR-A03	**1200**	7.0	**17**	**4.1**	0.7

[a] Anti-HIV-1 activity was determined using the amounts of p24 protein in the supernatants of the PHA-stimulated PBMC cultures using commercially available ELISA kit (Kodama et al., 2001). Bold indicates over 5-fold increase in EC_{50} value compared to HIV-1_{WT}.

[b] HIV-1_{NL4-3} and HIV-1_{KT} served as controls.

2.5. Determination of gp41 amino acid sequence

Nucleotide sequences of the clinical isolates were determined using an automated sequencer. Briefly, DNA was extracted from PBMCs infected with the clinical isolates, subjected to nested PCR for the gp41 coding region, and then directly sequenced as described previously (Nameki et al., 2005).

2.6. Measurement of circular dichroism (CD) spectra

N-HR peptides (N36, $N36_{V38A}$ or $N36_{N43D}$) and C-HR peptides (C34 or SC34EK) were incubated at 37 °C for 30 min (the final concentration of both the N-HR peptide and the C-HR peptide were 10 μM in pH 7.4, 12 mM phosphate-buffered solution containing 50 mM NaCl). The wavelength-dependence of molar ellipticity [θ] was monitored at 25 °C as the average of eight scans, and the thermal stability was estimated by monitoring the change in the CD signal at 222 nm in a spectropolarimeter (Model J-710; Jasco, Tokyo, Japan) equipped with a thermoelectric temperature controller. The midpoint of thermal unfolding transition (melting temperature [T_m]) of each complex was determined as described previously (Otaka et al., 2002). The percentages of a-helicity in 6-helix complexes were calculated by comparing the CD signal at 222 nm of N36/C34 or N36/SC34EK complexes in a spectropolarimeter.

2.7. Crystallization, data collection and refinement

Samples for crystallization were prepared by mixing solutions of N36 and SC34EK dissolved in 10 mM sodium acetate buffer at a concentration of 10 mg/mL. The mixture was incubated for 30 min at 37 °C, then was passed through a 22 μm filter. Crystallization was performed by the hanging drop vapor diffusion method at 4 °C. Droplets were prepared of equal amounts (2 μL) of reservoir solution and the peptide solution. Hexagonal prism crystals were obtained under the following conditions: 100 mM sodium acetate buffer (pH 4.0), 200 mM ammonium sulphate, 14% polyethylene glycol monomethyl ether 2000. After screening of

Table 3
Antiviral activity of HIV-1 gp41-derived peptides against HIV-2[a]

HIV-2 strain	EC_{50} (nM)				
	ddC	T-20	C34	SC34	SC34EK
WT[b]	404 ± 196	35 ± 17	3.2 ± 0.9	1.4 ± 0.7	0.7 ± 0.3
HIV-2_{EHO}[c]	925 ± 188	14 ± 3.0 (×0.4)	**639 ± 87 (×200)**	**68 ± 10 (×49)**	**17 ± 1.2** (×24)
HIV-2_{ROD}[d]	**1808 ± 927**	**176 ± 68 (×5)**	**>1000 (>×313)**	**251 ± 29 (×179)**	**115 ± 33** (×164)

[a] Anti-HIV-2 activity was determined using the MAGI assay. All data represent mean ± standard deviation obtained from the results of three independent experiments. Bold indicates over 5-fold increase in EC_{50} value compared to HIV-1_{WT}.
[b] HIV-1_{NL4-3} served as a wild-type virus.
[c] HIV-2_{EHO} was dual-tropic HIV-2.
[d] HIV-2_{ROD} was T-tropic HIV-2.

various cryo-conditions, the suitable condition was found to be the addition of 35% xylitol to the peptide solution and a slight increase in the amount of the precipitant (*ca* 14.5%). The obtained crystals were easily broken by direct transfer from the crystallization condition to the cryo-condition, but the transfer of the fragile crystals could be accomplished by gradual change in conditions using stepwise increase in the amount (0–35% in five steps) of the cryoprotectant.

Data were collected at a beamline BL38B1 of SPring-8. Collected data were processed using DENZO and SCALEPACK from the HKL2000 package (Otwinowski and Minor, 1997). A molecular replacement solution was found using AMoRe (Navaza, 2001), with a molecular model of the HIV-1 gp41 core structure (PDB code: 1AIK). Model refinements and reconstruction were performed using REFMAC5 (Murshudov et al., 1999) and XtalView (McRee, 1999). The final model was refined at a resolution of 2.1 Å, to a crystallographic *R* value of 0.213 and a free *R* value of 0.238. Detailed data collection and refinement statistics are summarized in Table 1. Atomic coordinates and structural factors have been deposited at the Protein Data Bank (PDB code:2Z2T).

3. Results

3.1. Anti-HIV-1 activity of SC34 and SC34EK

We examined the anti-HIV-1 activity of SC34 and SC34EK against not only HIV-1_{WT} but also T-20- and/or C34-resistant clones observed in vitro. SC34 and especially SC34EK that has aligned EK modification more effectively suppress HIV-1 infection compared to C34 and T-20 (Table 1). D36S/V38M substitutions in the gp41 region (HIV-$1_{D36S/V38M}$), and a five amino acid (FNSTW) deletion in the V4 region of gp120 (ΔV4) with L33S/N43K in the gp41 region (HIV-$1_{\Delta V4/L33S/N43K}$) were isolated in vitro (Fikkert et al., 2002; Rimsky et al., 1998). L33S was also selected during C34-resistant induction in vitro (Armand-Ugon et al., 2003). C34 and its derivatives effectively inhibit entry of these clones into the host cell. In particular, SC34EK maintained strong activity even against V38E containing clones, such as HIV-$1_{V38E/N42S}$ (Armand-Ugon et al., 2003), which showed cross-resistance to T-20, C34 and SC34. Reduction of activities by SC34 and SC34EK was moderate in HIV-$1_{\Delta FNSTW/L33S/N43K}$ that showed high level resistance to T-20 and C34. Next, we examined the antiviral activities of C34 derivatives against clones containing major primary mutations V38A and N43D, which are mutations frequently observed in T-20 resistant variants in vivo (Cabrera et al., 2006; Derdeyn et al., 2001; Menzo et al., 2004; Poveda et al., 2004; Poveda et al., 2002; Xu et al., 2005) (Table 1). SC34 reduced its antiviral activities against HIV-1_{N43D}, while SC34EK maintained its potent activity, indicating that when EK is bound with the complementary electrostatic interactions appropriately aligned SC34EK can effectively suppress the infection by various clones resistant to T-20 and C34 both in vitro and in vivo.

We further evaluated activities of SC34 and SC34EK against V3-substituted clones (Table 1). HIV-1_{V3-ADA} uses mainly the CCR5 co-receptor for its entry into the host cells and has been reported to moderate T-20 resistance (≈10 fold), compared to the CXCR4 using strain of HIV-1, which shows higher susceptibility to fusion inhibitors (Reeves et al., 2002). As reported, the susceptibility of HIV-1_{V3-ADA} to T-20 decreased, however, C34 and its derivatives maintained their activity against the same variant. Interestingly, in our experiments, HIV-$1_{V3-SF162}$, HIV-1_{V3-CH1} and HIV-1_{V3-CH2} also showed comparable susceptibility to T-20. These results indicate that sequence variations in the V3 region do not always correlate with the observed T-20 susceptibility and are not involved in the resistance to C34 and its derivatives.

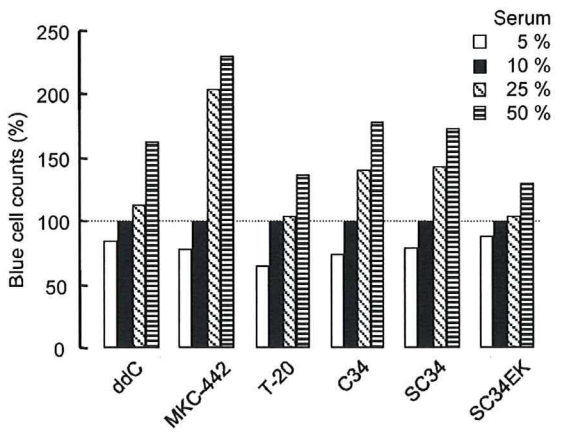

Fig. 3. Effect of FCS concentrations on anti-HIV-1 activity. Changes in the blue cell counts at various concentrations of FCS are shown. Blue cell counts at EC_{80} value in 10% FCS concentration (black bar) were used and set as 100%. White, black, hatched, and striped bars correspond to 5, 10, 25, and 50% FCS, respectively. Inhibitors for reverse transcriptase, ddC and MKC-442, and for fusion, T-20 were used as controls.

3.2. Amino acid sequence

Amino acid sequences of clinical isolates are shown in Fig. 2b. One isolate, HIV-1_{KT}, was obtained from a drug-naïve patient and the other three isolates (HIV-1_{411}, HIV-1_{412}, HIV-1_{A03}) were obtained from heavily drug-experienced patients. None of the patients had received T-20 therapy. Amino acid sequences of the N-HR were highly conserved within all HIV-1 clinical isolates with some small variations. In contrast, the N36 region of the two HIV-2 strains, EHO and ROD, was identical in both HIV-2 isolates. We found some variations in the amino acid sequences of the HIV-2 strains we isolated, as compared with the sequences deposited in the GenBank (accession number; M15390 and X05291 for HIV-2_{ROD}, and U272000 for HIV-2_{EHO}). Namely, we identified two different amino acids in the isolated HIV-2_{ROD}, V26L and

I157I/M (mixture of I and M), and one variation in the amino acid sequence of HIV-2_{EHO}, V45L. Except for I157M, other substitutions are observed in the majority of the HIV-2 strains, as reported in the HIV sequence database (Los Alamos National Laboratory: Los Alamos, NM, USA, http://www.hiv.lanl.gov). These substitutions might be introduced through different culture conditions, (e.g., host cells used for the propagation). We considered these substitutions as a polymorphism.

Sequence homology of the N36 region of the isolated HIV-1 strains was 31/36 (86%), including mutation D36G that is observed in the vast majority of HIV-1 strains (Kuiken et al., 2001). In contrast, those of the C34 region were relatively heterogeneous, 24/34 (71%) for HIV-1 and 12/34 (35%) for HIV-2. Sequence identity of the T-20 region (residues 117–152) in the HIV-1 strains was also variable 27/36 (75%), while in the HIV-2 strains the sequence identity was 15/36 (42%). These results indicate that even highly conserved two helical extracellular domain of the gp41 can allow polymorphisms.

3.3. Efficacy of the peptides against clinical isolates

To evaluate preclinical efficacy, we examined the antiviral activity of C34, SC34 and SC34EK against clinical isolates (Table 2). Replication of HIV-1_{NL4-3} and HIV-1_{KT}, a drug-naïve strain, was suppressed by all compounds tested. C34 showed decreased activity against HIV-$1_{IVR-A03}$, which was isolated from a heavily drug-exposed patient. SC34 also showed reduced susceptibility against three drug-experienced strains. However, it is difficult to conclude whether SC34 showed enhanced susceptibility against HIV-1_{KT} or reduced susceptibility against drug resistant strains. In contrast, T-20 and SC34EK suppressed the replication of all isolates tested to similar extents in EC_{50} values compared to HIV-1_{NL4-3} (Table 2), indicating that SC34EK with appropriately aligned EK residues effectively suppresses the replication of the clinical 3 isolates.

3.4. Anti-HIV-2 activity

To confirm the target specificity, we examined antiviral activities of SC34 and SC34EK against two HIV-2 strains, EHO and ROD. Compared to HIV-1_{NL4-3}, EHO and ROD contain 19 and 22 amino acid substitutions in the C34 region, respectively, and 15 amino acid substitutions in the N36 region, the anticipated site of binding of SC34 and SC34EK peptides (Fig. 2b). Like the parent peptide C34, both SC34 and SC34EK lost their potent activities (Table 3). Compared to HIV-1_{NL4-3}, 6 out of 19 residues in the C34 region of HIV-2_{EHO} and 7 out of 22 residues in the C34 region of HIV-2_{ROD} are located at positions *a*, *d*, and *e* that directly interact with the N36 binding surface. These substitutions in the N36 and C34 region in HIV-2 may be responsible for reduced anti-HIV-2 activities of the peptides derived from HIV-1. At present, we cannot conclude which amino acid substitutions are directly involved in the reduced susceptibility of the HIV-2 strain to the treatment with the peptide fusion inhibitor, and/or whether other regions besides the N36 and C34 regions might influence peptide susceptibility. However, our results indicate that SC34 and SC34EK maintain similar target specificity to the parent peptide, C34.

3.5. Effect of fetal calf serum (FCS) on anti-HIV-1 activity

To estimate the stability of the peptides in vivo, binding level of SC34EK, to serum components, (e.g., albumin) was examined. In this experiment, the antiviral activity in the presence of relatively high concentrations of fetal calf serum (FCS) was determined (Baba et al., 1993) (Fig. 3). EC_{80} values of the fusion inhibitors against HIV-1 replication in vitro were used. In the presence of 50% FCS, the activity of MKC-442 (I-EBU), a lipophilic non-nucleoside RT inhibitor, was reduced 2.3-fold compared with 10% FCS as described previously (Baba et al., 1993). However, the activities of SC34, SC34EK and T-20 were little influenced by serum components. Among the three, SC34EK was the least affected by the concentration of FCS.

We further examined the stability of peptide inhibitors in freshly prepared human sera ($n = 3$). After 1 h incubation of peptides in human sera (final concentration of 200 μM) at 37 °C, the anti-HIV-1 activity was examined using the MAGI assay. Comparable activities of all peptides tested were observed either with or without the incubation (data not shown). These results indicate that hydrophilic SC34EK likely retains its strong anti-HIV-1 activity in vivo, similarly to T-20, because of its low non-specific binding and protease cleavage in serum.

3.6. Peptide binding affinity

To clarify the mechanism of potent anti-HIV-1 activity observed with SC34EK, the binding affinity of SC34EK was evaluated by collecting the CD spectra using synthetic peptides. The CD spectra of equimolar mixtures of the N-HR and C-HR peptides showed spectrum minima at 208 and 222 nm, which indicate the presence of stable α-helical conformations. All combinations of peptides showed similar spectra at 25 °C, indicating that these peptides contained the same α-helicity (Fig. 4a), although the spectrum of C34 with N36 and N43D mutation ($N36_{N43D}$) indicated only weak α-helicity. These results indicate that N43D might reduce the stability of the conformation of the 6-helix bundle, thus decreasing the replication of HIV-1, whereas V38A does not. SC34EK formed stable 6-helix conformations with $N36_{V38A}$ and $N36_{N43D}$. Under these experimental conditions, wavelength-dependent spectra were similar with the exception of the spectrum of the $N36_{N43D}$/C34 complex. Thus, we analyzed thermal stabilities, defined as the midpoint of the thermal unfolding transition (T_m) values, of the potential 6-helix bundles of N-HR and C-HR peptides. T_m of N36/C34 was found to be 52.0 °C, while that of $N36_{V38A}$/C34 and $N36_{N43D}$/C34 decreased to 44.5 and 34.0 °C, respectively (Fig. 3b). In contrast, thermal stabilities of $N36_{V38A}$/SC34EK, $N36_{N43D}$/SC34EK and N36/SC34EK were much higher, 60.5, 56.0 and 69.5 °C, respectively. Thus, binding affinity of SC34EK to N-HR was stronger compared to that of C34. Alternatively, at the physiological temperature of 37 °C, only 60 and 40% of the α-helix content was observed in $N36_{V38A}$/C34 and $N36_{N43D}$/C34 mixtures, respectively, indicating that roughly half of C34 failed to form stably 6-helix bundle with the target N-HR harboring resistant mutations. Therefore, C34 reduces its anti-fusion activity exerted by dominant negative effect. In contrast, only 20% of the unfolded α-helix content was observed in SC34EK with mutated N36, which indicated that at 37 °C, binding of SC34EK to mutated N36 was comparable to that of C34 with wild-type N36 (Fig. 4b). Moreover, physiochemical properties of N-HR and SC34EK complexes, defined by T_m value, correlated well with their ability to inhibit HIV-1 fusion (Fig. 4c). These results suggest that the stability of the 6-helix complex, as judged by the binding stability (affinity), is directly correlated with the anti-HIV-1 activity.

3.7. Crystal structure of the N36/SC34EK complex

The crystal structure of the complex between SC34EK and the N-HR representative peptide N36 was resolved to a resolution of 2.1 Å (Table 4). In the asymmetric unit, a 6-helix bundle consisting of a central helix bundle of three N36 peptides surrounded by three SC34EK peptides was found. This arrangement is similar in the core structure of gp41 (Chan et al., 1997). Structural superimposition of the original gp41 core and the N36/SC34EK complex showed a good match, with an RMSD value of 0.59 for main-chain atoms

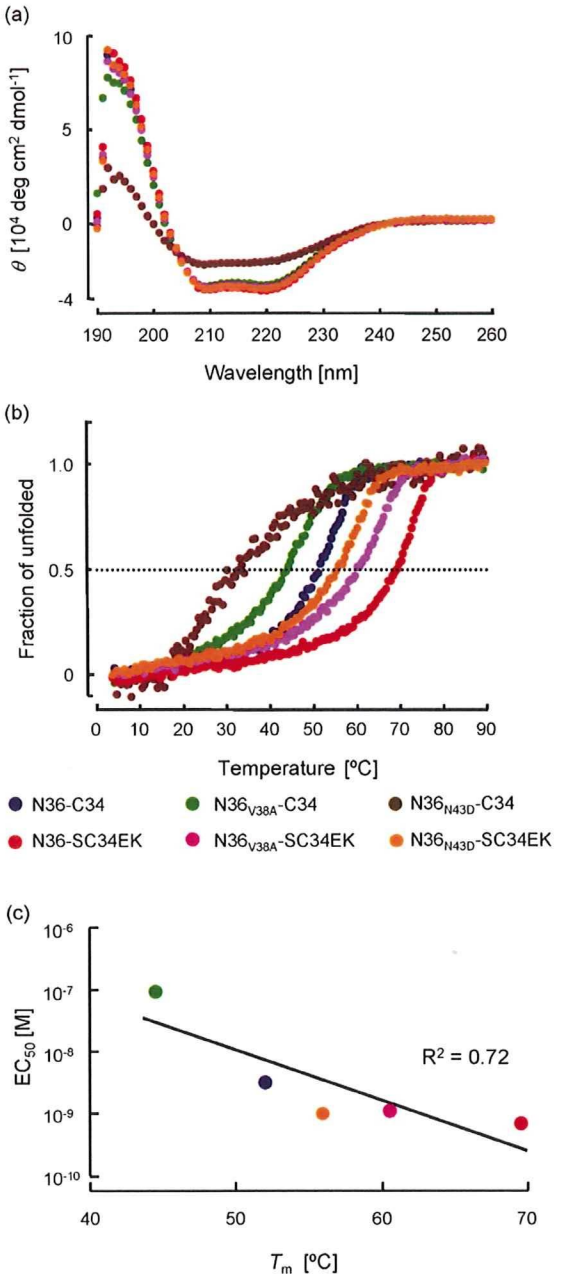

Fig. 4. CD analysis of peptide complex between resistant variants of N36 and C34 or SC34EK. (a) Wavelength-dependent CD spectra of the complexes in solution. The spectrum minima at 208 and 222 nm indicated the presence of stable α-helical conformations. (b) Thermal midpoint analysis was measured at 222 nm CD signal for the N and C peptide complexes. Final concentration of each peptide was 10 mM. The arrow indicates the physiological temperature of 37 C. (c) The correlation between T_m (b) and EC_{50} values (Table 1). Colors of plots correspond to those in panels (a) and (b). Combination of $N36_{N43D}$ and C34 (EC_{50} > 100 nM) is excluded.

(Fig. 5a and b). Hydrophobic contacts between SC34EK and N36 with tryptophan rich domain (WRD) and leucine zipper were preserved for the original gp41 core. All introduced charged residues of the EK motif were directed toward the solvent (Fig. 5c). As a direct consequence of introducing the EK motifs, the ratio of surface area occupied by charged residues to the total surface area was increased from 35% in the original molecule to 60% in the N36/SC34EK complex. Importantly, it appeared that tight bonding, such as ion pairing or hydrogen bonding, was not present in the

Table 4
Crystallization, data collection and refinement statistics

Data collection	BL38B1 Spring-8
Temperature (K)	100
Space group	$P3_121$
Cell dimensions *a*, *b*, *c* (Å)	105.01, 105.01, 78.31
Resolution limits (Å)	90.00–2.10
Number of unique reflections	29,461
Average redundancy	7.53
Completeness (%)	99.7
R_{merge}[a]	0.122
Refinement statistics	
Refinements resolution range (Å)	20.00–2.20
R/R_{free}[b] (%)	0.213/0.238
The highest resolution shell (Å)	2.15–2.10
R/R_{free}[b] (%)	0.231/0.255
RMSD from ideal	
Bonds (Å)	0.010
Angles (°)	1.015
⟨*B*⟩ for atomic model[c] (Å²)	29.93
Ramachandran plot	
Most favored regions (%)	100

[a] $R_{merge} = \sum|I_h - \langle I_h\rangle| / \sum I_h$, where $\langle I_h\rangle$ is the average intensity of reflection *h* and symmetry-related reflections.

[b] *R* and $R_{free} = \sum||F_o| - |F_c|| / \sum|F_o|$ calculated for reflections of the working set and test (5%) set, respectively.

[c] ⟨*B*⟩ is the average temperature factor for all protein atoms.

side-chains of the residues of the EK motif. Electrostatic interaction may involve in constrained structure which provides the enhanced α-helicity observed (Fig. 4). This structural analysis demonstrated that the interaction between N36 and SC34EK retained the ability to form the 6-helix bundle structure despite the substitution of more than one third of the residues (13/34) in the sequence of SC34EK.

4. Discussion

In this study, we characterized a novel α-helical peptide, SC34EK that effectively inhibits replication of HIV-1 strains resistant to T-20 and C34. The activity was specific to HIV-1 and little influenced by serum components. We demonstrate that the potent anti-HIV-1 activity of SC34EK is derived from its high affinity to the N-HR region by the CD analysis. Further, we reveal that SC34EK binds to its target, N-HR in identical manner that C34 does by the structure analysis.

The structural analysis of the N36/SC34EK complex clearly demonstrated that the interaction between SC34EK and N36 peptides was maintained by hydrophobic contacts and that the EK motif was directed toward the solvent. The introduction of the EK residues increased the proportion of accessible surface area occupied by charged residues. Although tight bonding was not observed, a continuous electrostatic potential between the EK residues may serve to stabilize the helix bundle. Such helix stabilization, which might occur on the surface of the HIV-1 virion between SC34EK and the N36 region of gp41, could result in the high anti-HIV-1 activity. In this regard, SC34EK, containing an aligned EK motif, showed more potent anti-HIV-1 activity compared to SC34, which has one misaligned EK motif (Fig. 2a). Increasing the hydrophilic surface area may prevent aggregation of SC34EK as compared to parental peptide C34. Therefore, SC34EK might distribute into the various organs in the body without being trapped and destroyed in the reticular systems or having its activity reduced by non-specific binding to proteins (e.g., albumin) (Fig. 3).

We further demonstrate that SC34EK specifically binds to the target, N-HR of HIV-1, since it only exerted weak activity to two

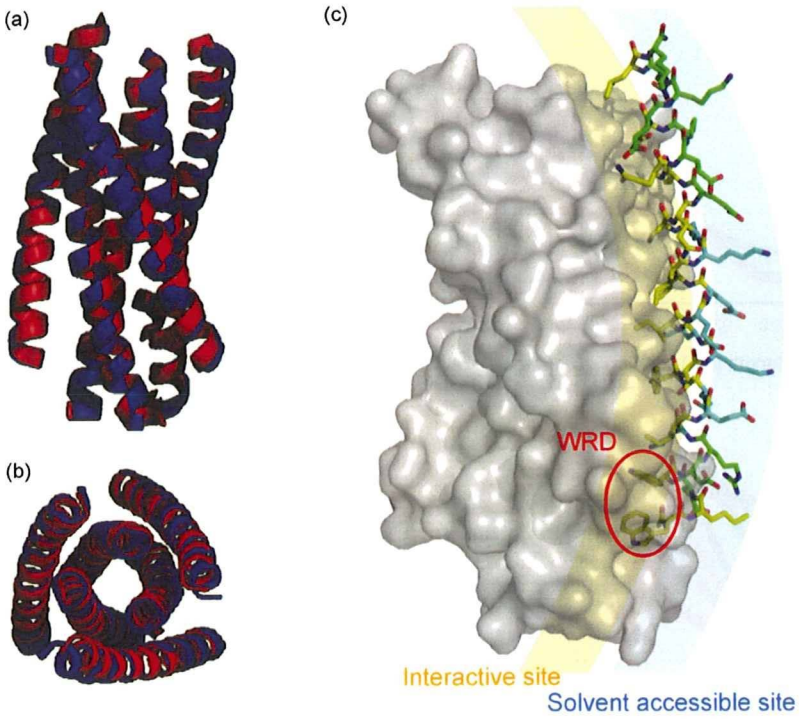

Fig. 5. Structure of the 6-helix bundle formed by N36 and SC34EK. (a and b) The gp41 core structure and N36/SC34EK complex are shown in red and blue, respectively. (c) Stick model representation of SC34EK. The stick model of SC34EK is shown, and three N36s in the core and two other surrounded SC34EK are represented in gray. SC34EK showed amphiphilic properties. The location of the N-terminal tryptophan rich domain (WRD) in SC34EK is indicated by a red circle. Original and introduced charged amino acids are indicated in green and blue, respectively.

HIV-2 strains that contain 15 amino acid substitutions in the N-HR compared to HIV-1 NL4-3 strain (Table 3 and Fig. 2b). These results suggest that to develop resistance to SC34EK, at least, certain mutations in not only the N-HR but also the C-HR are required to be introduced. This might delay emergence of resistant HIV-1 variants to SC34EK in vivo.

So far, some approaches for stabilizing α-helix structures through the introduction of artificial amino acids were reported for HIV-1 fusion inhibitors T-20 (Judice et al., 1997) and C34 (Sia et al., 2002), including an example of an amino acid containing terminal olefin-derived side chains, designed as a substrate for the ring-closing olefin metathesis (Blackwell et al., 2001) and an example of a hydrocarbon-stapled peptides (Phelan et al., 1997) Walensky et al. (2004) applied a hydrocarbon-stapled modification to generate peptides that bind to the BH3 helical domain of Bcl-2, an anti-apoptotic protein, and demonstrated that a synthesized peptide mimic that binds to the BH3 domain activates apoptosis in leukemic cells. However, all peptides exerted only moderate activity in vivo, although they showed efficient binding to the target proteins in vitro (Blackwell et al., 2001; Judice et al., 1997; Sia et al., 2002; Walensky et al., 2004). It is likely that during the formation of the 6-helix bundle and the fusion process, gp41 changes its conformation drastically, suggesting that a flexible conformation of the peptide may be required to preserve actual inhibition. Compared with tethered, constrained peptides, EK modification that facilitates electrostatic stabilization displays such flexibility while exhibiting enhanced α-helicity. Most recently, T290676, a 38 amino acid peptide, has been reported to suppress various fusion inhibitor-resistant strains of HIV-1 (Dwyer et al., 2007). Like SC34EK, T290676 is substituted with the charged and hydrophilic amino acids, glutamic acid (E) and arginine (R), at the solvent accessible site and shows potent anti-HIV-1 activity.

In conclusion, we have demonstrated that SC34EK selectively inhibits various HIV-1 strains, including T-20 resistant clones, through increased stability of the α-helix. The sequence of the solvent accessible site of α-helical peptides is replaceable and modifications of this sequence can regulate α-helicity with target specificity. Therefore, our approach of introducing the EK motif in the α-helical structure of the peptide inhibitor will help to generate future peptide inhibitors with high anti-HIV efficacy and potentially fewer adverse effects.

Acknowledgements

This work was supported in part by grants for the Promotion of AIDS Research from the Ministry of Health and Welfare and for the Ministry of Education, Culture, Sports, Science, and Technology (MEXT) of Japan (E.K. and S.O.); a grant for Research for Health Sciences Focusing on Drug Innovation from the Japan Health Sciences Foundation (E.K., S.O., N.F. and M.M.), the Program of Founding Research Centers for Emerging and Reemerging Infectious Diseases by the MEXT (S.N.), a Health and Labor Sciences Research Grant for Research on HIV/AIDS from the Ministry of Health and Labor of Japan (S.N.), and the 21st Century COE program (H.N., K.K., K.I. and N.F.). H.N. is grateful for the JSPS Research Fellowships for Young Scientists. Appreciation is expressed to Mr. Maxwell Reback (Kyoto University) for reading this manuscript.

References

Aquaro S, D'Arrigo R, Svicher V, Perri GD, Caputo SL, Visco-Comandini U, et al. Specific mutations in HIV-1 gp41 are associated with immunological success in HIV-1-infected patients receiving enfuvirtide treatment. J Antimicrob Chemother 2006;58:714–22.

Armand-Ugon M, Gutierrez A, Clotet B, Este JA. HIV-1 resistance to the gp41-dependent fusion inhibitor C-34. Antiviral Res 2003;59:137–42.

Baba M, Yuasa S, Niwa T, Yamamoto M, Yabuuchi S, Takashima H, et al. Effect of human serum on the in vitro anti-HIV-1 activity of 1-[(2-hydroxyethoxy)methyl]-6-(phenylthio)thymine (HEPT) derivatives as related to their lipophilicity and serum protein binding. Biochem Pharmacol 1993;45:2507–12.
Baldwin CE, Berkhout B. Second site escape of a T20-dependent HIV-1 variant by a single amino acid change in the CD4 binding region of the envelope glycoprotein. Retrovirology 2006;3:84.
Blackwell HE, Sadowsky JD, Howard RJ, Sampson JN, Chao JA, Steinmetz WE, et al. Ring-closing metathesis of olefinic peptides: design, synthesis, and structural characterization of macrocyclic helical peptides. J Org Chem 2001;66:5291–302.
Cabrera C, Marfil S, Garcia E, Martinez-Picado J, Bonjoch A, Bofill M, et al. Genetic evolution of gp41 reveals a highly exclusive relationship between codons 36, 38 and 43 in gp41 under long-term enfuvirtide-containing salvage regimen. AIDS 2006;20:2075–80.
Chan DC, Chutkowski CT, Kim PS. Evidence that a prominent cavity in the coiled coil of HIV type 1 gp41 is an attractive drug target. Proc Natl Acad Sci U S A 1998;95:15613–7.
Chan DC, Fass D, Berger JM, Kim PS. Core structure of gp41 from the HIV envelope glycoprotein. Cell 1997;89:263–73.
Chan DC, Kim PS. HIV entry and its inhibition. Cell 1998;93:681–4.
Derdeyn CA, Decker JM, Sfakianos JN, Wu X, O'Brien WA, Ratner L, et al. Sensitivity of human immunodeficiency virus type 1 to the fusion inhibitor T-20 is modulated by coreceptor specificity defined by the V3 loop of gp120. J Virol 2000;74:8358–67.
Derdeyn CA, Decker JM, Sfakianos JN, Zhang Z, O'Brien WA, Ratner L, et al. Sensitivity of human immunodeficiency virus type 1 to fusion inhibitors targeted to the gp41 first heptad repeat involves distinct regions of gp41 and is consistently modulated by gp120 interactions with the coreceptor. J Virol 2001;75:8605–14.
Dwyer JJ, Wilson KL, Davison DK, Freel SA, Seedorff JE, Wring SA, et al. Design of helical, oligomeric HIV-1 fusion inhibitor peptides with potent activity against enfuvirtide-resistant virus. Proc Natl Acad Sci U S A 2007;104:12772–7.
Ferrer M, Kapoor TM, Strassmaier T, Weissenhorn W, Skehel JJ, Oprian D, et al. Selection of gp41-mediated HIV-1 cell entry inhibitors from biased combinatorial libraries of non-natural binding elements. Nat Struct Biol 1999;6:953–60.
Fikkert V, Cherepanov P, Van Laethem K, Hantson A, Van Remoortel B, Pannecouque C, et al. env chimeric virus technology for evaluating human immunodeficiency virus susceptibility to entry inhibitors. Antimicrob Agents Chemother 2002;46:3954–62.
Foda M, Harada S, Maeda Y. Role of V3 independent domains on a dual-tropic human immunodeficiency virus type 1 (HIV-1) envelope gp120 in CCR5 coreceptor utilization and viral infectivity. Microbiol Immunol 2001;45:521–30.
Judice JK, Tom JY, Huang W, Wrin T, Vennari J, Petropoulos CJ, et al. Inhibition of HIV type 1 infectivity by constrained alpha-helical peptides: implications for the viral fusion mechanism. Proc Natl Acad Sci U S A 1997;94:13426–30.
Kajiwara K, Kodama E, Matsuoka M. A novel colorimetric assay for CXCR4 and CCR5 tropic human immunodeficiency viruses. Antivir Chem Chemother 2006;17:215–23.
Kimpton J, Emerman M. Detection of replication-competent and pseudotyped human immunodeficiency virus with a sensitive cell line on the basis of activation of an integrated beta-galactosidase gene. J Virol 1992;66:2232–9.
Kodama EI, Kohgo S, Kitano K, Machida H, Gatanaga H, Shigeta S, et al. 4′-Ethynyl nucleoside analogs: potent inhibitors of multidrug-resistant human immunodeficiency virus variants in vitro. Antimicrob Agents Chemother 2001;45:1539–46.
Kuiken C, Foly B, Hahn B, Marx P, McCutchan F, Mellors J, et al.Kuiken C, Foly B, Hahn B, Marx P, McCutchan F, Mellors J, Wolinsky S, Korber B, editors. HIV Sequence Compendium 2001. Los Alamos, NM: Los Alamos National Laboratory; 2001.
Lalezari JP, Henry K, O'Hearn M, Montaner JS, Piliero PJ, Trottier B, et al. Enfuvirtide, an HIV-1 fusion inhibitor, for drug-resistant HIV infection in North and South America. N Engl J Med 2003;348:2175–85.
Lazzarin A, Clotet B, Cooper D, Reynes J, Arasteh K, Nelson M, et al. Efficacy of enfuvirtide in patients infected with drug-resistant HIV-1 in Europe and Australia. N Engl J Med 2003;348:2186–95.
Liu S, Lu H, Niu J, Xu Y, Wu S, Jiang S. Different from the HIV fusion inhibitor C34, the anti-HIV drug fuzeon (T-20) inhibits HIV-1 entry by targeting multiple sites in gp41 and gp120. J Biol Chem 2005;280:11259–73.
Maeda Y, Foda M, Matsushita S, Harada S. Involvement of both the V2 and V3 regions of the CCR5-tropic human immunodeficiency virus type 1 envelope in reduced sensitivity to macrophage inflammatory protein 1alpha. J Virol 2000;74:1787–93.
Maeda Y, Venzon DJ, Mitsuya H. Altered drug sensitivity, fitness, and evolution of human immunodeficiency virus type 1 with pol gene mutations conferring multi-dideoxynucleoside resistance. J Infect Dis 1998;177:1207–13.
Marqusee S, Baldwin RL. Helix stabilization by Glu-.Lys+ salt bridges in short peptides of de novo design. Proc Natl Acad Sci U S A 1987;84:8898–902.
Matthews T, Salgo M, Greenberg M, Chung J, DeMasi R, Bolognesi D. Enfuvirtide: the first therapy to inhibit the entry of HIV-1 into host CD4 lymphocyte. Nat Rev Drug Discov 2004;3:215–25.
McRee DE. XtalView/Xfit—a versatile program for manipulating atomic coordinates and electron density. J Struct Biol 1999;125:156–65.
Menzo S, Castagna A, Monachetti A, Hasson H, Danise A, Carini E, et al. Genotype and phenotype patterns of human immunodeficiency virus type 1 resistance to enfuvirtide during long-term treatment. Antimicrob Agents Chemother 2004;48:3253–9.
Mink M, Mosier SM, Janumpalli S, Davison D, Jin L, Melby T, et al. Impact of human immunodeficiency virus type 1 gp41 amino acid substitutions selected during enfuvirtide treatment on gp41 binding and antiviral potency of enfuvirtide in vitro. J Virol 2005;79:12447–54.
Murshudov GN, Vagin AA, Lebedev A, Wilson KS, Dodson EJ. Efficient anisotropic refinement of macromolecular structures using FFT. Acta Crystallogr 1999;D55:247–55.
Nameki D, Kodama E, Ikeuchi M, Mabuchi N, Otaka A, Tamamura H, et al. Mutations conferring resistance to human immunodeficiency virus type 1 fusion inhibitors are restricted by gp41 and Rev-responsive element functions. J Virol 2005;79:764–70.
Navaza J. Implementation of molecular replacement in AMoRe. Acta Crystallogr 2001;D57(Pt 10):1367–72.
Otaka A, Nakamura M, Nameki D, Kodama E, Uchiyama S, Nakamura S, et al. Remodeling of gp41-C34 peptide leads to highly effective inhibitors of the fusion of HIV-1 with target cells. Angew Chem Int Ed Engl 2002;41:2937–40.
Otwinowski Z, Minor W. Processing of X-ray diffraction data collected in oscillation mode. Met Enzymol 1997;276:307–26.
Phelan JC, Skelton NJ, Braisted AC, McDowell RS. A general method for constraining short peptides to an alpha-helical conformation. J Am Chem Soc 1997;119:455–60.
Poveda E, Rodes B, Labernardiere JL, Benito JM, Toro C, Gonzalez-Lahoz J, et al. Evolution of genotypic and phenotypic resistance to Enfuvirtide in HIV-infected patients experiencing prolonged virologic failure. J Med Virol 2004;74:21–8.
Poveda E, Rodes B, Toro C, Martin-Carbonero L, Gonzalez-Lahoz J, Soriano V. Evolution of the gp41 env region in HIV-infected patients receiving T-20, a fusion inhibitor. AIDS 2002;16:1959–61.
Reeves JD, Gallo SA, Ahmad N, Miamidian JL, Harvey PE, Sharron M, et al. Sensitivity of HIV-1 to entry inhibitors correlates with envelope/coreceptor affinity, receptor density, and fusion kinetics. Proc Natl Acad Sci U S A 2002;99:16249–54.
Rimsky LT, Shugars DC, Matthews TJ. Determinants of human immunodeficiency virus type 1 resistance to gp41-derived inhibitory peptides. J Virol 1998;72:986–93.
Salzwedel K, West JT, Hunter E. A conserved tryptophan-rich motif in the membrane-proximal region of the human immunodeficiency virus type 1 gp41 ectodomain is important for Env-mediated fusion and virus infectivity. J Virol 1999;73:2469–80.
Sia SK, Carr PA, Cochran AG, Malashkevich VN, Kim PS. Short constrained peptides that inhibit HIV-1 entry. Proc Natl Acad Sci U S A 2002;99:14664–9.
Walensky LD, Kung AL, Escher I, Malia TJ, Barbuto S, Wright RD, et al. Activation of apoptosis in vivo by a hydrocarbon-stapled BH3 helix. Science 2004;305:1466–70.
Wei X, Decker JM, Liu H, Zhang Z, Arani RB, Kilby JM, et al. Emergence of resistant human immunodeficiency virus type 1 in patients receiving fusion inhibitor (T-20) monotherapy. Antimicrob Agents Chemother 2002;46:1896–905.
Weiner MP, Costa GL, Schoettlin W, Cline J, Mathur E, Bauer JC. Site-directed mutagenesis of double-stranded DNA by the polymerase chain reaction. Gene 1994;151:119–23.
Wild C, Oas T, McDanal C, Bolognesi D, Matthews T. A synthetic peptide inhibitor of human immunodeficiency virus replication: correlation between solution structure and viral inhibition. Proc Natl Acad Sci U S A 1992;89:10537–41.
Xu L, Pozniak A, Wildfire A, Stanfield-Oakley SA, Mosier SM, Ratcliffe D, et al. Emergence and evolution of enfuvirtide resistance following long-term therapy involves heptad repeat 2 mutations within gp41. Antimicrob Agents Chemother 2005;49:1113–9.
Xu Y, Hixon MS, Dawson PE, Janda KD. Development of a FRET assay for monitoring of HIV gp41 core disruption. J Org Chem 2007;72:6700–7.

ELSEVIER

INSTITUT PASTEUR

Microbes and Infection 11 (2009) 334–343

www.elsevier.com/locate/micinf

Original article

Phenotypic studies on recombinant human immunodeficiency virus type 1 (HIV-1) containing CRF01_AE *env* gene derived from HIV-1-infected patient, residing in central Thailand

Piraporn Utachee [a,1], Piyamat Jinnopat [a,1], Panasda Isarangkura-na-ayuthaya [b,1], U. Chandimal de Silva [a,c], Shota Nakamura [a,c], Uamporn Siripanyaphinyo [a,c], Nuanjun Wichukchinda [b], Kenzo Tokunaga [d], Teruo Yasunaga [a,c], Pathom Sawanpanyalert [b], Kazuyoshi Ikuta [a,e], Wattana Auwanit [b], Masanori Kameoka [a,e,*]

[a] *Thailand–Japan Research Collaboration Center on Emerging and Re-emerging Infections (RCC-ERI),[2] Nonthaburi 11000, Thailand*
[b] *National Institute of Health, Department of Medical Sciences, Ministry of Public Health, Nonthaburi 11000, Thailand*
[c] *Department of Genome Informatics, Research Institute for Microbial Diseases, Osaka University, Osaka 565-0871, Japan*
[d] *Department of Pathology, National Institute of Infectious Diseases, Tokyo 162-8640, Japan*
[e] *Department of Virology, Research Institute for Microbial Diseases, Osaka University, Osaka 565-0871, Japan*

Received 30 October 2008; accepted 11 December 2008
Available online 27 December 2008

Abstract

Human immunodeficiency virus type 1 (HIV-1) *env* genes were cloned from blood samples of HIV-1-infected Thai patients, and 35 infectious CRF01_AE envelope glycoprotein (Env)-recombinant viruses were established. In this report, we examined the neutralization susceptibility of these viruses to human monoclonal antibodies, 2G12, IgG1 b12, 2F5 and 4E10, pooled patient plasma, coreceptor antagonists and fusion inhibitor, T-20. The neutralization susceptibility of CRF01_AE Env-recombinant viruses to 2F5, 4E10, patient plasma, coreceptor antagonists and T-20 varied, while most viruses showed low susceptibility to 2G12 and IgG1 b12. Several dual-tropic viruses showed lower susceptibility to 2F5 and 4E10 than CXCR4- or CCR5-tropic viruses. Neutralization susceptibility of the CRF01_AE Env-recombinant virus to pooled patient plasma was negatively correlated with the length of the V1/V2 region or the number of potential N-linked glycosylation sites in conserved regions of gp120. No correlation was found between the coreceptor usage and neutralization susceptibility of the virus to T-20, whereas several dual-tropic viruses showed higher susceptibility to coreceptor antagonists than CXCR4- or CCR5-tropic viruses. We propose that these CRF01_AE Env-recombinant viruses are useful to further study the molecular mechanism of the susceptibility of CRF01_AE Env to neutralizing antibodies and viral entry inhibitors.

Keywords: HIV-1; HIV envelope glycoprotein gp120; HIV envelope glycoprotein gp41; HIV entry inhibitors; Neutralization tests

1. Introduction

Human immunodeficiency virus type 1 (HIV-1) is characterized by extensive genetic heterogeneity [1]. Due to this variability, HIV-1 is subdivided into three groups, M (major), O (outlying) and N (new or non-M, non-O). The viruses in group M, which are responsible for the majority of infections in the worldwide HIV-1 epidemic, are further classified into many subtypes or circulating recombinant forms (CRFs).

* Corresponding author. RCC-ERI, 6th floor, Building 10, Department of Medical Sciences, Ministry of Public Health, Tiwanon Road, Muang, Nonthaburi 11000, Thailand. Tel.: +66 2 965 9748; fax: +66 2 965 9749.
E-mail address: mkameoka@biken.osaka-u.ac.jp (M. Kameoka).
[1] These authors equally contributed to this work.
[2] RCC-ERI was established by the Research Institute for Microbial Diseases, Osaka University, Japan and the Department of Medical Sciences, Ministry of Public Health, Thailand.

1286-4579/$ - see front matter © 2008 Elsevier Masson SAS. All rights reserved.
doi:10.1016/j.micinf.2008.12.008

While subtype B of HIV-1 is the predominant subtype in the Americas, Europe and Australia, the growing epidemic of non-B subtypes is found in Africa and Asia [2].

The envelope glycoproteins (Env), gp120 and gp41, are the most variable HIV-1 proteins with typical intersubtype and intrasubtype differences soaring to 35% and 20%, respectively [1]. HIV-1 Env plays a central role in viral transmission, and mediates attachment and incorporation of the virus into target cells through specific interaction with the CD4 receptor and chemokine coreceptors [3]. In addition, HIV-1 Env is the major target of antibody-mediated neutralization, and thus is a candidate viral protein to elicit humoral immune responses in HIV-1 vaccine development [4]. Recent HIV-1 epidemiologic data show that non-B subtypes are more prevalent than subtype B in developing regions of the world [2] where a protective vaccine against HIV-1 infection is needed urgently. Therefore, more information on the Env of non-B subtypes is required, although virological and immunobiochemical studies on HIV-1 Env have been performed extensively using subtype B viruses.

CRF01_AE is one of the major HIV-1 subtypes that dominate the global epidemic, and is prevalent throughout Southeast Asia [2]. In particular, this subtype is responsible for more than 95% of infection cases in Thailand, Cambodia and Viet Nam [2]. Although immunological and virological studies on CRF01_AE Env have previously been performed elsewhere [5–8], most were performed using viruses isolated in the early or mid-1990s. In other words, information on the Env of currently circulating CRF01_AE viruses is still limited. We previously cloned HIV-1 *env* genes from blood samples of HIV-1-infected Thai patients in 2006, and established 35 CRF01_AE Env-recombinant viruses [9]. In this report, phenotypic studies of these CRF01_AE Env-recombinant viruses were performed.

2. Materials and methods

2.1. Preparation of CRF01_AE Env-recombinant viruses

HIV-1 *env* genes were amplified from uncultured peripheral blood mononuclear cells (PBMC), plasma and *in vitro* isolated virus derived from HIV-1-infected, drug treatment-naïve patients residing in central Thailand in 2006 [9]. Blood samples were used with approval from the institutional ethics committee of the Research Institute for Microbial Diseases, Osaka University as well as from the Department of Medical Sciences, Ministry of Public Health of Thailand. Amplified *env* gene was cloned into the pNL4-3- [10] derived luciferase reporter virus, pNL-envCT [11], and 35 infectious CRF01_AE Env-recombinant viruses were generated [9]. In addition, the recombinant viruses containing the partial fragments of CRF01_AE *env* genes 65CC1 and 65CC4 were constructed, as follows. The BspEI–XbaI fragment, encoding the Env signal peptide and the N-terminal regions of gp120 (C1, V1, V2, C2, V3 and most C3 regions), of 65CC1 or 65CC4 as well as the XbaI–NotI fragment, encoding the C-terminal regions of gp120 (14 amino acids of C3, V4, C4, V5 and C5 regions) and gp41, of 65CC4 or 65CC1 was cloned into pNL-envCT, respectively. Moreover, PCR-amplified gp120 gene of 101PL1 or 98PB2 as well as PCR-amplified gp41 gene of 98PB2 or 101PL1 was cloned into pNL-envCT, respectively, as described previously [11]. Viral supernatants were prepared by transfecting 293T cells with the viral construct using FuGENE 6 transfection reagent (Roche), essentially as described [12]. pNL-envCT and pNL-Luc-BaLenv [12], which contains the *env* gene of pBa-L (GenBank accession no. AB253432), were used to prepare CXCR4-tropic (X4) and CCR5-tropic (R5) subtype B HIV-1, respectively. The viral titer was determined by measuring the concentration of HIV-1 Gag p24 antigen in viral supernatants by enzyme-linked immunosorbent assay (ELISA) (Vironostika HIV-1 Antigen Microelisa System, bioMérieux, Boxtel, The Netherlands).

2.2. Study on protein structure-related properties of 35 CRF01_AE env genes

Nucleotide and deduced amino acid sequences of 35 CRF01_AE *env* genes were previously determined [9]. Amino acid residues of gp120 variable regions, V1, V2, V3, V4 and V5, were counted manually. In addition, the potential N-linked glycosylation (PNLG) site was examined using *N*-glycosite (www.hiv.lanl.gov), and PNLG sites in gp120 and gp41 as well as in the variable and conserved regions of gp120 were counted manually.

2.3. Neutralization assay

Neutralization susceptibilities of CRF01_AE Env-recombinant virus were examined for neutralizing human monoclonal antibody (NHMAb) against gp120, 2G12 [13] and IgG1 b12 [14]; NHMAb against gp41, 2F5 [15] and 4E10 [16]; heat-inactivated (56 °C for 1 h) pooled patient plasma; CXCR4 antagonist, AMD3100 (Sigma–Aldrich, St. Louis, MO); CCR5 antagonist, TAK-779 [17]; and fusion inhibitor, T-20 [18]. Briefly, viral supernatant (2 ng of p24 antigen) was treated with 2-fold serially diluted NHMAbs or pooled patient plasma at 37 °C for 30 min. Alternatively, U87.CD4.CXCR4 or U87.CD4.CCR5 cells [19] were treated with 2-fold serially diluted AMD3100, TAK-779 or T-20. U87.CD4.CXCR4 cells were used as target cells for X4 and X4R5 viruses, whereas U87.CD4.CCR5 cells were used as target cells for R5 and X4R5 viruses. Cells and viral supernatant were mixed and incubated for 48 h, and then luciferase activity in infected cells was measured using Steady Glo Luciferase assay kit (Promega) with LB960 microplate luminometer (Berthold, Bad Wildbad, Germany). As a negative control for pooled patient plasma, the plasma of 8 healthy donors was pooled and subjected to the control experiment. The neutralization level was evaluated as a reduction in luciferase activity in infected cells. The 50% inhibitory concentration (IC50) of NHMAbs, AMD3100, TAK-779 and T-20 for suppressing viral replication, and the reciprocal plasma dilution, at which viral

replication was suppressed by 50% (50% inhibitory dilution, ID50), were calculated by the dose–response curve using a standard function of GraphPad Prism 5 software (GraphPad Software, San Diego, CA). 2G12, 2F5 and 4E10 (provided by Dr. Hermann Katinger) as well as IgG1 b12 (provided by Dr. Dennis Burton and Dr. Carlos Barbas), TAK-779, T-20 (provided by Roche), U87.CD4.CXCR4 and U87.CD4.CCR5 (provided by Dr. HongKui Deng and Dr. Dan R. Littman) were obtained through the AIDS Research and Reference Reagent Program, Division of AIDS, NIAID, NIH.

2.4. Statistical analysis

Statistical analysis was carried out using the standard function of GraphPad Prism 5 software with an unpaired *t* test or Pearson's *r* correlation test.

3. Results

3.1. Protein structure-related properties of 35 CRF01_AE env genes

We previously established 35 infectious CRF01_AE Env-recombinant viruses, including 6 X4, 23 R5 and 6 dual-tropic (X4R5) viruses [9]. The recombinant virus containing the CRF01_AE *env* gene derived from uncultured PBMC, plasma or *in vitro* isolated virus was denoted as PB, PL or CC, respectively (Table 1). These recombinant viruses showed a variety of infectivity [9]. We examined the protein structure-related properties, including the length of gp120 variable regions and the number of PNLG sites, for the deduced amino acid sequence of 35 CRF01_AE *env* genes determined previously [9]. Variation was observed in the length of gp120 variable regions, V1, V2, V4 and V5, as well as in the number

Table 1
Source, coreceptor usage and structure-related properties of 35 functional CRF01_AE *env* genes.

env gene	Source of *env* gene	Coreceptor usage[a]	Number of amino acid residues[b]					Number of PNLG sites[b,c]	
			V1	V2	V3	V4	V5	gp120	gp41
21PL2	Plasma	R5	28	52	35	25	10	25	4
22PL1	Plasma	R5	31	43	35	20	7	24	4
29CC1	Isolated virus	X4R5	29	40	35	28	8	23	4
41PB3	PBMC	X4R5	30	46	35	24	11	24	4
41CC1	Isolated virus	X4R5	35	46	35	25	11	27	3
45PB1	PBMC	X4R5	31	41	35	28	8	25	5
45CC1	Isolated virus	X4R5	30	41	35	28	8	26	4
47PL1	Plasma	R5	29	43	35	31	6	24	5
47CC11	Isolated virus	R5	29	47	35	31	5	25	4
50PB2	PBMC	X4R5	29	48	35	28	8	23	5
50PL1	Plasma	R5	29	48	35	28	8	22	5
52PB3	PBMC	R5	38	44	35	20	9	25	4
52PL4	Plasma	R5	38	44	35	20	8	24	4
52PL7	Plasma	R5	38	40	35	20	7	26	4
55PL1	Plasma	R5	34	47	35	27	9	23	6
60PB2	PBMC	R5	38	42	35	20	10	24	5
60PL2	Plasma	R5	38	42	35	20	10	24	6
60CC3	Isolated virus	X4	27	39	35	20	9	23	5
62PL1	Plasma	R5	29	41	35	25	9	24	5
65PL1	Plasma	R5	28	52	35	31	13	23	4
65CC1	Isolated virus	X4	31	58	34	31	21	26	4
65CC4	Isolated virus	X4	29	45	34	31	14	24	4
98PB2	PBMC	R5	50	40	35	32	7	24	3
98CC2	Isolated virus	X4	33	64	35	32	10	30	4
98CC3	Isolated virus	X4	32	41	35	25	8	23	4
99PB2	PBMC	R5	31	52	34	26	7	23	4
99PL2	Plasma	R5	31	52	35	29	7	20	4
99CC8	Isolated virus	R5	29	51	35	18	7	25	4
101PL1	Plasma	R5	28	44	35	32	8	26	4
102CC2	Isolated virus	R5	39	59	35	21	8	25	5
104PB4	PBMC	R5	31	38	35	28	11	27	4
105PB1	PBMC	R5	32	40	35	27	10	23	4
105PL2	Plasma	R5	29	51	35	18	7	26	4
105PL3	Plasma	R5	32	40	35	27	10	23	4
107CC2	Isolated virus	X4	32	39	35	31	9	22	4

[a] Coreceptor usage of the CRF01_AE Env was determined by the infectivity of CRF01_AE Env-recombinant virus in U87.CD4.CXCR4 (U87.X4) and U87.CD4.CCR5 (U87.R5) cells, as described previously [9].

[b] Amino acid residues in gp120 variable regions, V1, V2, V3, V4 and V5 and PNLG sites in the deduced amino acid sequence of CRF01_AE *env* genes [9] were counted manually.

[c] PNLG sites were examined using *N*-glycosite (www.hiv.lanl.gov).

of PNLG sites in gp120 and gp41 (Table 1). In addition, the number of PNLG sites in variable and conserved regions of gp120 varied among 35 CRF01_AE *env* genes (data not shown).

3.2. Neutralization susceptibility of CRF01_AE Env-recombinant virus to NHMAbs against gp120 or gp41 as well as to pooled patient plasma

We examined the neutralization susceptibility of CRF01_AE Env-recombinant viruses to NHMAbs against gp120, 2G12 and IgG1 b12; and NHMAbs against gp41, 2F5 and 4E10. IgG1 b12 recognizes the CD4 binding domain [20], while 2G12 recognizes a mannose cluster [21]. In addition, 2F5 and 4E10 recognize two adjacent conserved epitopes located on the membrane-proximal ectodomain of gp41 [8,22]. Plasma from 19 patients with CD4 counts ranging from 7 to 584 cells/mm^3, from whom *env* genes were amplified [9], was pooled and employed in the neutralization test. The results showed that most of the 35 CRF01_AE Env-recombinant viruses replicated efficiently even in the presence of 2G12 or IgG1 b12 at the highest concentration tested in this study (5 μg/ml) (Table 2). These results suggest that CRF01_AE Env is not susceptible to NHMAbs against gp120 elicited in HIV-1 subtype B-infected patients. Only the CRF01_AE Env-recombinant virus containing the *env* gene, 65CC1, showed high susceptibility to IgG1 b12, whereas the recombinant virus containing 65CC4 showed low susceptibility to IgG1 b12 (Table 2). Although 65CC1 and 65CC4 were amplified from an individual blood sample [9], these CRF01_AE Env showed different susceptibility to IgG1 b12 (Table 2). In order to further study the high susceptibility of 65CC1 to IgG1 b12, the recombinant viruses containing the partial fragments of 65CC1 and 65CC4 were constructed and tested for their neutralization susceptibility to IgG1 b12. The results showed that the CRF01_AE Env-recombinant virus containing the N-terminal regions of 65CC1 (65CC1N4C) showed high susceptibility to IgG1 b12, while the recombinant virus containing the C-terminal regions of 65CC1 (65CC4N1C) showed low susceptibility to IgG1 b12 (Table 3).

We next studied the neutralization susceptibility of the CRF01_AE Env-recombinant virus to NHMAbs against gp41, 2F5 and 4E10. The results showed that most CRF01_AE Env-recombinant viruses showed high susceptibility to 4E10, whereas approximately (approx.) 40% of recombinant viruses showed high susceptibility to 2F5 (Table 2, with IC50 less than 1 μg/ml). Several CRF01_AE Env-recombinant viruses showed higher susceptibility to 2F5 and 4E10 than the recombinant virus containing either subtype B X4 (pNL4-3) or R5 (pBa-L) Env (Table 2). In addition, the susceptibility of several X4R5 viruses to 2F5 and 4E10 was higher in neutralization tests using U87.CD4.CCR5 cells as target cells, compared with tests using U87.CD4.CXCR4 cells (Table 2). These results suggested that 2F5 and 4E10 reacted more effectively with gp41 of X4R5 viruses in the process of viral entry mediated by CCR5 coreceptor compared with viral entry mediated by CXCR4 coreceptor.

We next performed neutralization tests using pooled patient plasma. The results showed that the susceptibility to pooled patient plasma varied among 35 CRF01_AE Env-recombinant viruses (Table 2). Two CRF01_AE Env-recombinant viruses containing the *env* gene, 55PL1 or 101PL1, showed particularly higher susceptibility to pooled patient plasma compared with the remaining 33 recombinant viruses (Table 2). In contrast, pooled plasma from 8 healthy donors showed no neutralization activity for the CRF01_AE Env-recombinant virus (data not shown). 101PL1 and 98PB2 showed highest and lowest susceptibility to pooled patient plasma, respectively (Table 2). In order to further study the high susceptibility of 101PL1 to patient plasma, we constructed the recombinant viruses containing the gp120 gene of 101PL1 or 98PB2 as well as the gp41 gene of 98PB2 or 101PL1, respectively, and tested the neutralization susceptibility of these recombinant viruses. The results showed that the recombinant virus containing gp120 of 101PL1 showed significantly high susceptibility to pooled patient plasma (data not shown), suggesting that gp120 is responsible for the high susceptibility of 101PL1 to patient plasma.

3.3. Study on the correlation between coreceptor usage and the susceptibility of the CRF01_AE Env-recombinant virus to neutralizing antibodies

No correlation was observed between viral infectivity [9] and the neutralization susceptibility of the CRF01_AE Env-recombinant virus to 2F5, 4E10 or pooled patient plasma (data not shown). We then examined the correlation between coreceptor usage and the neutralization susceptibility of CRF01_AE Env-recombinant virus to these antibodies. The results showed that several X4R5 viruses were less susceptible to 2F5 or 4E10 compared with X4 or R5 viruses (Fig. 1A, B). In contrast, no correlation was observed between coreceptor usage and the neutralization susceptibility of CRF01_AE Env-recombinant virus to pooled patient plasma (Fig. 1C).

3.4. Study of the correlations between the susceptibility of CRF01_AE Env-recombinant virus to neutralizing antibodies and protein structure-related properties of CRF01_AE Env

We next examined the correlations between the susceptibility of CRF01_AE Env-recombinant virus to 2F5, 4E10 or pooled patient plasma and the length of the gp120 variable regions or the number of PNLG sites in CRF01_AE Env. No correlations were observed between the neutralization susceptibility of CRF01_AE Env-recombinant virus to 2F5 or 4E10 and the length of the gp120 variable regions or the number of PNLG sites (data not shown). In contrast, we found correlations between the susceptibility of CRF01_AE Env-recombinant virus to pooled patient plasma and the protein structure-related properties of CRF01_AE Env, as follows. Two CRF01_AE Env-recombinant viruses containing the *env* gene, 55PL1 or 101PL1, showed distinctly high neutralization susceptibility to pooled patient plasma compared with the

Table 2
Neutralization susceptibilities of CRF01_AE Env-recombinant virus to NHMAbs against gp120 or gp41 as well as to pooled patient plasma.[a]

env gene	Coreceptor usage	Target cells	IC50 of NHMAb (μg/ml)[b]				ID50 of pooled patient plasma[b]
			2G12	IgG1 b12	2F5	4E10	
pNL4-3[c]	X4	U87.X4	0.69	0.36	0.47	2.35	368
pBa-L[c]	R5	U87.R5	0.16	0.06	1.49	1.70	242
21PL2	R5	U87.R5	>5[d]	>5	1.29	0.52	65
22PL1	R5	U87.R5	>5	>5	0.21	0.11	317
29CC1	X4R5	U87.X4	>5	>5	>5	0.56	252
		U87.R5	>5	>5	>5	0.18	280
41PB3	X4R5	U87.X4	>5	>5	>5	0.71	168
		U87.R5	>5	>5	1.01	0.24	155
41CC1	X4R5	U87.X4	>5	>5	>5	0.65	99
		U87.R5	>5	>5	>5	2.12	61
45PB1	X4R5	U87.X4	>5	>5	>5	1.48	130
		U87.R5	>5	>5	2.03	0.67	107
45CC1	X4R5	U87.X4	>5	>5	>5	2.54	150
		U87.R5	>5	>5	>5	0.57	131
47PL1	R5	U87.R5	>5	>5	>5	1.58	44
47CC11	R5	U87.R5	>5	>5	>5	0.80	64
50PB2	X4R5	U87.X4	>5	>5	1.76	0.54	351
		U87.R5	>5	>5	1.87	0.26	282
50PL1	R5	U87.R5	>5	>5	0.66	0.36	111
52PB3	R5	U87.R5	>5	>5	1.41	1.20	238
52PL4	R5	U87.R5	>5	>5	0.85	0.58	128
52PL7	R5	U87.R5	>5	>5	0.45	0.03	321
55PL1	R5	U87.R5	>5	>5	0.76	0.33	1395
60PB2	R5	U87.R5	>5	>5	0.30	0.10	128
60PL2	R5	U87.R5	>5	>5	1.58	1.07	23
60CC3	X4	U87.X4	>5	>5	>5	0.28	303
62PL1	R5	U87.R5	>5	>5	0.34	0.22	72
65PL1	R5	U87.R5	>5	>5	>5	0.65	113
65CC1	X4	U87.X4	>5	0.69	>5	0.10	268
65CC4	X4	U87.X4	>5	>5	0.23	0.41	201
98PB2	R5	U87.R5	>5	>5	>5	0.13	18
98CC2	X4	U87.X4	>5	>5	>5	0.80	36
98CC3	X4	U87.X4	>5	>5	>5	0.13	39
99PB2	R5	U87.R5	>5	>5	0.07	0.11	59
99PL2	R5	U87.R5	>5	>5	>5	0.70	127
99CC8	R5	U87.R5	>5	>5	0.27	0.18	25
101PL1	R5	U87.R5	>5	>5	>5	0.02	3529
102CC2	R5	U87.R5	>5	>5	1.35	0.23	31
104PB4	R5	U87.R5	>5	>5	>5	0.27	36
105PB1	R5	U87.R5	>5	>5	0.39	0.24	423
105PL2	R5	U87.R5	>5	>5	0.10	0.21	30
105PL3	R5	U87.R5	>5	>5	0.52	0.52	409
107CC2	X4	U87.X4	>5	>5	0.18	0.10	189

[a] Neutralization susceptibility of X4 or R5 virus was examined using U87.CD4.CXCR4 (U87.X4) or U87.CD4.CCR5 (U87.R5) cells, respectively, whereas that of X4R5 virus was examined using both cell lines.

[b] IC50 of NHMAbs for suppressing viral replication and the reciprocal dilution of pooled patient plasma at which viral replication was suppressed by 50% (50% inhibitory dilution, ID50) were calculated using GraphPad Prism 5 software.

[c] Recombinant virus containing subtype B X4 (pNL4-3) or R5 (pBa-L) Env.

[d] IC50 is >5 μg/ml.

remaining 33 recombinant viruses (Table 2), and we could not fully elucidate the mechanism underlying such high susceptibility of these recombinant viruses to patient plasma in this study; therefore, the following results were obtained from studies on the remaining 33 CRF01_AE Env-recombinant viruses. The neutralization susceptibility of CRF01_AE Env-recombinant virus was negatively correlated with the length of V1/V2 (V1 plus V2) (Fig. 1D) or of the V1–V4 region (including V1, V2, C2, V3, C3 and V4 regions in this order) (Fig. 1E), but not with the length of V1 (data not shown), V2 (data not shown) or the V4 (Fig. 1F) region. In addition, the neutralization susceptibility of CRF01_AE Env-recombinant virus was negatively correlated with the number of PNLG sites in gp160 (Fig. 1G), gp120 (data not shown) and C1/C2/C3 (C1 plus C2 plus C3) regions (Fig. 1H), but not with the number of PNLG sites in the V1–V4 (Fig. 1I), V1/V2 (data not shown) or V4 region (data not shown). Negative correlations were especially observed between the susceptibility of CRF01_AE Env-recombinant virus to pooled patient plasma and the length of the V1/V2 region (Fig. 1D) or the number of PNLG sites in

Table 3
Neutralization susceptibility of CRF01_AE Env-recombinant virus containing the partial fragments of 65CC1 and 65CC4 to IgG1 b12.[a]

env gene	IC50 of IgG1 b12 (μg/ml)[b]
65CC1	0.70 ± 0.16
65CC4	>5[c]
65CC1N4C[d]	0.86 ± 0.40
65CC4N1C[e]	>5

[a] Neutralization susceptibility of the recombinant virus was examined using U87.CD4.CXCR4 cells.

[b] IC50 of IgG1 b12 for suppressing viral replication was calculated using GraphPad Prism 5 software. Data are shown as the means and standard deviations of three independent experiments.

[c] IC50 is >5 μg/ml.

[d] Recombinant virus containing the N-terminal regions of 65CC1 and the C-terminal regions of 65CC4.

[e] Recombinant virus containing the N-terminal regions of 65CC4 and the C-terminal regions of 65CC1.

the C1/C2/C3 region (Fig. 1H). These results suggested that the neutralization susceptibility of CRF01_AE Env to pooled patient plasma was at least partly regulated by the length of the V1/V2 region as well as by the number of PNLG sites in the conserved regions of gp120.

3.5. Neutralization susceptibility of CRF01_AE Env-recombinant virus to CXCR4 and CCR5 antagonists as well as to fusion inhibitor, T-20

During the HIV-1 entry process, Env gp120 interacts with CD4 and then with CXCR4 or CCR5 coreceptor [3], and the interaction between gp120 and coreceptor is inhibited by small-molecule antagonists of CXCR4 and CCR5 [17,23]. In addition, Env gp41 mediates fusion between viral and cellular membranes [3], and this fusion process is inhibited by a fusion inhibitor, T-20 [18,23]. We next studied the neutralization

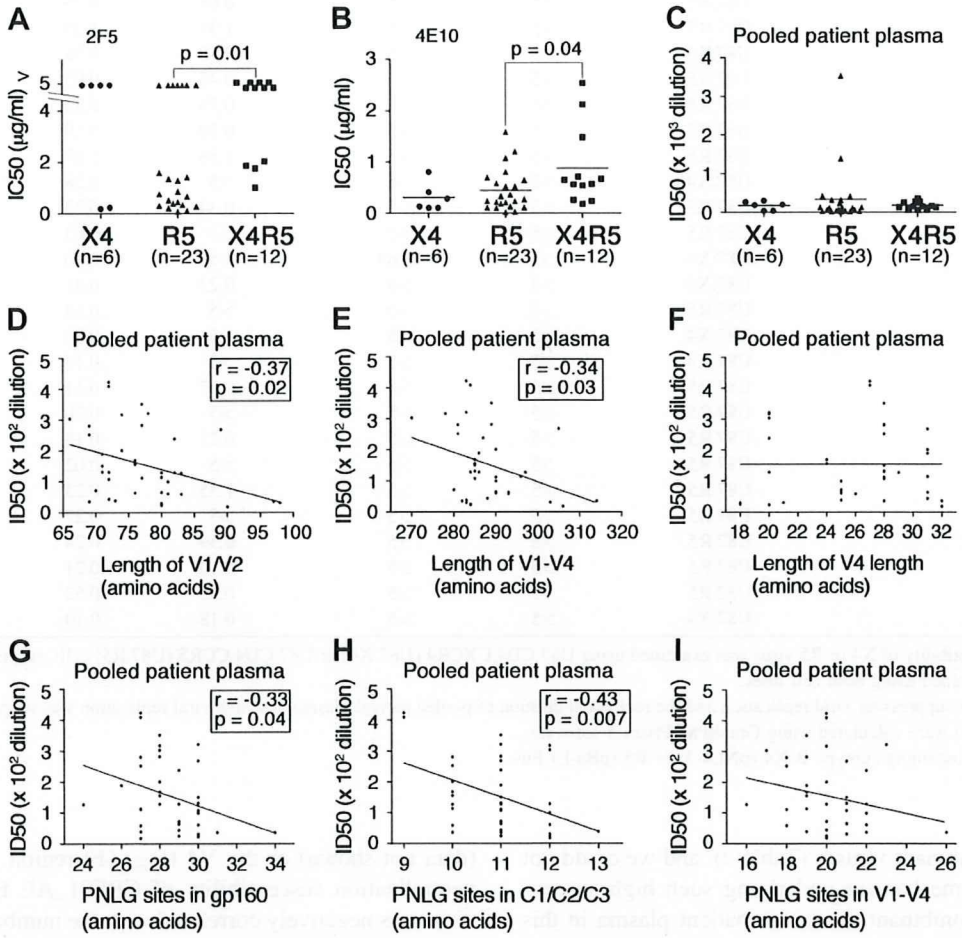

Fig. 1. Correlations between susceptibility of CRF01_AE Env-recombinant virus to neutralizing antibodies and the coreceptor usage or protein structure-related properties of CRF01_AE Env. Neutralization susceptibility of CRF01_AE Env-recombinant virus to the indicated antibody or pooled patient plasma was determined, as described in Materials and methods. Neutralization susceptibility of the CRF01_AE Env-recombinant virus to 2F5 (A), 4E10 (B) or pooled patient plasma (C) was compared among viruses with different coreceptor usage. In addition, correlations were examined between the neutralization susceptibility of the CRF01_AE Env-recombinant virus to pooled patient plasma and the length of indicated variable regions of gp120 (D–F) or the number of PNLG sites in the indicated Env regions (G–I). In panels A–C, horizontal solid lines show median values, and the number of samples studied (n) is shown below the panels. Differences among groups were analyzed by the unpaired t test, and are reported when $P < 0.05$. In panels D–I, correlations were evaluated using Pearson's r correlation test, and the correlation coefficient (r) is reported when $P < 0.05$.

Table 4
Neutralization susceptibilities of CRF01_AE Env-recombinant virus to AMD3100, TAK-779 and T-20.[a]

env gene	Coreceptor usage	Target cells	IC50 (nM)[b]		
			AMD3100	TAK-779	T-20
pNL4-3[c]	X4	U87.X4	7.7	ND	65.0
pBa-L[c]	R5	U87.R5	ND[d]	5.0	7.5
21PL2	R5	U87.R5	ND	3.7	50.0
22PL1	R5	U87.R5	ND	2.3	32.5
29CC1	X4R5	U87.X4	2.8	ND	30.0
		U87.R5	ND	1.2	45.0
41PB3	X4R5	U87.X4	3.5	ND	10.0
		U87.R5	ND	1.1	5.0
41CC1	X4R5	U87.X4	5.1	ND	65.0
		U87.R5	ND	2.4	20.0
45PB1	X4R5	U87.X4	6.3	ND	67.5
		U87.R5	ND	4.4	22.5
45CC1	X4R5	U87.X4	7.5	ND	102.5
		U87.R5	ND	1.0	57.5
47PL1	R5	U87.R5	ND	7.8	97.5
47CC11	R5	U87.R5	ND	1.3	55.0
50PB2	X4R5	U87.X4	1.7	ND	35.0
		U87.R5	ND	0.2	5.0
50PL1	R5	U87.R5	ND	6.9	10.0
52PB3	R5	U87.R5	ND	4.9	75.0
52PL4	R5	U87.R5	ND	0.5	210.0
52PL7	R5	U87.R5	ND	2.3	47.5
55PL1	R5	U87.R5	ND	3.3	42.5
60PB2	R5	U87.R5	ND	5.4	87.5
60PL2	R5	U87.R5	ND	2.9	80.0
60CC3	X4	U87.X4	15.8	ND	47.5
62PL1	R5	U87.R5	ND	3.7	17.5
65PL1	R5	U87.R5	ND	3.4	17.5
65CC1	X4	U87.X4	7.4	ND	10.0
65CC4	X4	U87.X4	10.3	ND	20.0
98PB2	R5	U87.R5	ND	0.7	22.5
98CC2	X4	U87.X4	6.1	ND	65.0
98CC3	X4	U87.X4	12.6	ND	15.0
99PB2	R5	U87.R5	ND	11.8	45.0
99PL2	R5	U87.R5	ND	4.0	12.5
99CC8	R5	U87.R5	ND	18.1	57.5
101PL1	R5	U87.R5	ND	14.6	1.0
102CC2	R5	U87.R5	ND	4.2	30.0
104PB4	R5	U87.R5	ND	5.3	32.5
105PB1	R5	U87.R5	ND	3.6	17.5
105PL2	R5	U87.R5	ND	9.5	35.0
105PL3	R5	U87.R5	ND	1.3	15.0
107CC2	X4	U87.X4	17.4	ND	45.0

[a] Neutralization susceptibility of X4 or R5 virus was examined using U87.CD4.CXCR4 (U87.X4) or U87.CD4.CCR5 (U87.R5) cells, respectively, whereas that of X4R5 virus was examined using both cell lines.
[b] IC50 of AMD3100, TAK-779 and T-20 for suppressing viral replication was calculated using GraphPad Prism 5 software.
[c] Recombinant virus containing subtype B X4 (pNL4-3) or R5 (pBa-L) Env.
[d] Not done.

susceptibility of 35 CRF01_AE Env-recombinant viruses to CXCR4 antagonist, AMD3100; CCR5 antagonist, TAK-779; and fusion inhibitor, T-20. AMD3100 was tested for X4 and X4R5 viruses, whereas TAK-779 was tested for R5 and X4R5 viruses. In addition, T-20 was tested for X4, R5 and X4R5 viruses. Neutralization susceptibility to those compounds varied among 35 CRF01_AE Env-recombinant viruses, and there were approx. 9-, 90- or 210-fold differences in the susceptibility to AMD3100, TAK-779 or T-20, respectively, between CRF01_AE Env-recombinant virus showing the highest and lowest susceptibility to the respective compound (Table 4).

3.6. Study of the correlation between coreceptor usage and the neutralization susceptibility of CRF01_AE Env-recombinant virus to AMD3100, TAK-779 or T-20

No correlations were observed between viral infectivity [9] and the neutralization susceptibility of CRF01_AE Env-recombinant virus to AMD3100, TAK-779 or T-20 (data not shown). We then examined the correlation between coreceptor usage and the neutralization susceptibility of CRF01_AE Env-recombinant virus to these compounds. The results showed that the neutralization susceptibility of several X4R5 viruses to AMD3100 (Fig. 2A) or TAK-779 (Fig. 2B) was higher than that of X4 or R5 viruses, respectively, indicating that the X4R5 virus was neutralized more efficiently by coreceptor antagonists than X4 or R5 virus. In contrast, there was no apparent correlation between coreceptor usage and the susceptibility of CRF01_AE Env-recombinant virus to T-20 (Fig. 2C).

3.7. Study of the correlations between the susceptibility of CRF01_AE Env-recombinant virus to AMD3100, TAK-779 or T-20 and protein structure-related properties of CRF01_AE Env

No correlations were observed between the neutralization susceptibility of CRF01_AE Env-recombinant virus to AMD3100, TAK-779 or T-20 and the length of gp120 variable regions or the number of PNLG sites (data not shown).

4. Discussion

In this report, we examined the susceptibility of 35 CRF01_AE Env-recombinant viruses to neutralizing antibodies, coreceptor antagonists and a fusion inhibitor. In addition, possible correlations between the neutralization susceptibility of the recombinant virus and coreceptor usage or the protein structure-related properties of CRF01_AE Env were examined.

Most CRF01_AE Env-recombinant viruses showed low susceptibility to two NHMAbs against gp120, IgG1 b12 and 2G12 (Table 2), similar to subtype C Env-recombinant viruses [24]. In contrast, the recombinant virus containing either subtype B X4 (pNL4-3) or R5 (pBa-L) Env showed high susceptibility to IgG1 b12 and 2G12 (Table 2). IgG1 b12 and 2G12 recognize conformational epitopes, as follows. IgG1 b12 recognizes the CD4 binding domain [20], and the reactivity of HIV-1 Env to IgG1 b12 is affected by mutations in the V2–C3 region (including V2, C2, V3 and C3 regions in this order) [25]. In addition, 2G12 recognizes a mannose cluster [21]. Although PNLG sites recognized by 2G12 [21] were highly conserved among 35 CRF01_AE *env* genes (data not shown), all CRF01_AE Env-recombinant viruses showed low susceptibility to neutralization by 2G12 (Table 2). Thus, it is

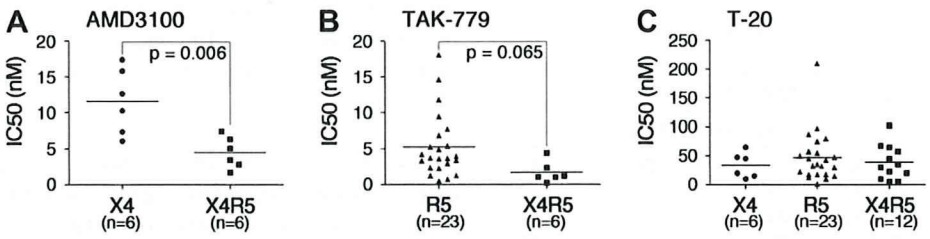

Fig. 2. Correlations between coreceptor usage and the neutralization susceptibility of the CRF01_AE Env-recombinant virus to coreceptor antagonists or fusion inhibitor, T-20. Neutralization susceptibility of the CRF01_AE Env-recombinant virus to the indicated compound was determined, as described in Materials and methods. Neutralization susceptibility of the CRF01_AE Env-recombinant virus to AMD3100 (A), TAK-779 (B) or T-20 (C) was compared among viruses with different coreceptor usage. Horizontal solid lines show median values, and the number of samples studied (*n*) is shown below the panels. Differences among groups were analyzed with the unpaired *t* test, and are reported when $P < 0.05$.

suggested that the protein structure, including conformation of the CD4 binding domain, is somehow different between CRF01_AE and subtype B Env gp120. The CRF01_AE Env-recombinant virus containing the *env* gene, 65CC1, showed high susceptibility to IgG1 b12, exceptionally among 35 CRF01_AE Env-recombinant viruses, whereas the recombinant virus containing the *env* gene, 65CC4, showed low susceptibility to IgG1 b12. Two *env* genes, 65CC1 and 65CC4, were derived from an individual blood sample, and thus showed a close phylogenetic relationship [9]; however, several amino acid residues as well as PNLG sites differed between the deduced amino acid sequences of 65CC1 and 65CC4 [9]. Neutralization tests of the recombinant viruses containing the partial fragments of 65CC1 and 65CC4 revealed that the N-terminal regions of gp120, consisted of the C1, V1, V2, C2, V3 and most of C3 regions, were responsible for the high susceptibility of 65CC1 to IgG1 b12 (Table 3). Thirty-one amino acid residues in these regions, including 6, 19 and 1 amino acid residues in the V1, V2 and V3 regions, respectively, differed between 65CC1 and 65CC4 (data not shown). In addition, 65CC4 contained a few additional PNLG sites in the V1/V2 region compared to 65CC1 (data not shown). N-linked glycan is known to account for approx. 50% of the molecular mass of HIV-1 Env and to affect the neutralization susceptibility of this glycoprotein [26]. Therefore, we consider that the structural features of gp120 V1/V2 region, including the existence of these PNLG sites, might play important role in determining the neutralization susceptibility of CRF01_AE viruses to IgG1 b12. Further studies are currently ongoing to elucidate the molecular mechanism and explain the different susceptibility of two CRF01_AE *env* genes to IgG1 b12.

Thirty-five CRF01_AE Env-recombinant viruses showed significant variations in their neutralization susceptibility to 2F5, 4E10 and pooled patient plasma (Table 2). The core epitopes of 2F5 (ELDKWA) [22] and 4E10 (NWFDIT) [8] were conserved in approx. 60% of CRF01_AE Env-recombinant viruses [9]. Several CRF01_AE Env-recombinant viruses, in which the core epitopes of 2F5 and 4E10 were conserved, showed high susceptibility to those NHMAbs, and vice versa (data not shown); however, many exceptions were also found, as follows. On one hand, the CRF01_AE Env-recombinant virus containing the *env* gene, 41CC1, 45CC1, 98PB2, 98CC3 and 104PB4, showed low susceptibility to 2F5 (Table 2), although the core epitope of 2F5 was conserved [9]. On the other hand, recombinant viruses containing the *env* gene, 55PL1 and 60PB2 or 29CC1, 55PL1, 60CC3, 98CC3, 99PB2, 99CC8, 105PL2 and 107CC2, showed high susceptibility to 2F5 or 4E10, respectively (Table 2), although the core epitopes of those NHMAbs contained amino acid substitutions such as E151Q (amino acid substitution from glutamic acid to glutamine at position 151 in gp41), A156T, N160D/S, D163N/S or T165S [9]. In addition, recombinant viruses containing the *env* gene, 45PB1, 47PL1 and 60PL2, which contained the PNLG site in the core epitope region of 4E10 [9], showed relatively low susceptibility to 4E10, whereas the recombinant virus containing the *env* gene, 55PL1, showed high susceptibility to 4E10 (Table 2), even though the PNLG site was introduced into the core epitope region [9]. Taken together, these results suggested that the susceptibility of CRF01_AE Env to 2F5 and 4E10 was not determined by the conservation of core epitope sequences or the existence of the PNLG site within core epitope regions. Similar results were reported previously on subtype B viruses [27], and we considered that other structural features of Env gp120 and/or gp41 may affect the neutralization susceptibility of HIV-1 Env to NHMAbs against gp41. The neutralization susceptibility of CRF01_AE Env-recombinant virus to pooled patients plasma was negatively correlated with the length of the V1/V2 region (Fig. 1D) or the number of PNLG sites in the C1/C2/C3 region (Fig. 1H). These negative correlations were statistically significant, but the values of the correlation coefficient were low, suggesting that other structural features of CRF01_AE Env may also play roles to determine the neutralization susceptibility of CRF01_AE viruses. Nevertheless, our results suggest that the V1/V2 region plays, at least in part, an important role in regulating the susceptibility of CRF01_AE viruses to neutralizing antibodies, similar to subtypes B [28] and C [29] viruses. In addition, our results also suggest that N-linked glycan plays a negative role as a glycan shield, reducing the susceptibility of CRF01_AE viruses to neutralizing antibodies.

Thirty-five CRF01_AE Env-recombinant viruses showed various levels of neutralization susceptibility to coreceptor antagonists or fusion inhibitor, T-20 (Table 4). We observed a tendency for the neutralization susceptibility of X4R5 viruses to AMD3100 or TAK-779 to be higher than that of X4 or R5 viruses, respectively (Fig. 2A, B). Although the